PERGAMON

Quaternary Science Reviews 22 (2003) 1597–1629

QSR

Orbital insolation, ice volume, and greenhouse gases

William F. Ruddiman*

Department of Environmental Sciences, University of Virginia, Clark Hall, Charlottesville, VA 22903, USA

Received 11 March 2002; accepted 24 February 2003

Abstract

The SPECMAP models of orbital-scale climate change (Imbrie et al., Paleoceanography 7 (1992) 701, Paleoceanography 8 (1993) 699) are the most comprehensive to date: all major climatic observations were analyzed within the framework of the three orbital signals. Subsequently, tuning of signals in Vostok ice to insolation forcing has fixed the timing of greenhouse-gas changes closely enough to permit an assessment of their orbital-scale climatic role. In addition, evidence from several sources has suggested changes in the SPECMAP $\delta^{18}O$ time scale. This new information indicates that the timing of CO_2 changes at the periods of precession and obliquity does not fit the 1992 SPECMAP model of a "train" of responses initiated in the north, propagated to the south, and later returning north to force the ice sheets. In addition, analysis of the effects of rectification on 100,000-year climatic signals reveals that all have a phase on or near that of eccentricity. This close clustering of phases rules out the long time constants for 100,000-year ice sheets required by the 1993 SPECMAP model.

A new hypotheses presented here revives elements of an earlier CLIMAP view (Hays et al., Science 194 (1976a) 1121) but adds a new assessment of the role of greenhouse gases.

As proposed by Milankovitch, summer (mid-July) insolation forces northern hemisphere ice sheets at the obliquity and precession periods, with an ice time constant derived here of 10,000 years. Changes in ice volume at 41,000 years drive ice-proximal signals (SST, NADW, dust) that produce a strong positive CO_2 feedback and further amplify ice-volume changes. At the precession period, July insolation forces ice sheets but it also drives fast and early responses in CH_4 through changes in tropical monsoons and boreal wetlands, and variations in CO_2 through southern hemisphere processes. These CH_4 and CO_2 responses enhance insolation forcing of ice volume.

Climatic responses at 100,000 years result from eccentricity pacing of forced processes embedded in obliquity and precession cycles. Increased modulation of precession by eccentricity every 100,000 years produces 23,000-year CO_2 and CH_4 maxima that enhance ablation caused by summer insolation and drive climate deeper into an interglacial state. When eccentricity modulation decreases at the 100,000-year cycle, ice sheets grow larger in response to obliquity forcing and activate a 41,000-year CO_2 feedback that drives climate deeper into a glacial state. Alternation of these forced processes because of eccentricity pacing produces the 100,000-year cycle. The 100,000-year cycle began 0.9 Myr ago because gradual global cooling allowed ice sheets to survive during weak precession insolation maxima and grow large enough during 41,000-year ice-volume maxima to generate strong positive CO_2 feedback.

The natural orbital-scale timing of these processes indicates that ice sheets should have appeared 6000–3500 years ago and that CO_2 and CH_4 concentrations should have fallen steadily from 11,000 years ago until now. But new ice did not appear, and CO_2 and CH_4 began anomalous increases at 8000 and 5000 years ago, respectively. Human generation of CO_2 and CH_4 is implicated in these anomalous trends and in the failure of ice sheets to appear in Canada.

0. Introduction

Many factors affect climate change at orbital time scales, including external forcing (insolation) and the resulting changes in ice volume and greenhouse gases that produce interactions within the climate system. The SPECMAP group has produced the most comprehensive analysis to date of orbital-scale climate change, based on insolation changes dated by astronomy and marine $\delta^{18}O$ records that serve both as an ice-volume proxy and a time-correlative signal to link regional responses (Imbrie et al., 1992, 1993). Only SPECMAP has attempted to explain the origin of all major climatic responses recorded in Earth's archives within a

*Fax: +1-804-982-2137.

E-mail address: wfr5c@virginia.edu, rudds2@ntelos.net (W.F. Ruddiman).

0277-3791/03/$ - see front matter
doi:10.1016/S0277-3791(03)00087-8

framework that isolates each of the three orbital signals: obliquity, precession, and eccentricity. For this reason, the SPECMAP models of climate change are the focus of this paper.

As explained in Section 1, however, the SPECMAP legacy actually left two strikingly different views of the mechanisms of orbital-scale climate change. The earlier view, originating during the CLIMAP era (Hays et al., 1976a; Imbrie and Imbrie, 1980), and still implicit in the early SPECMAP work of Imbrie et al. (1984), accepted the Milankovitch (1941) hypothesis that summer insolation in the northern hemisphere at the periods of obliquity and precession directly forces ice sheets through changes in summer ablation. In contrast, the view proposed in the final SPECMAP models (Imbrie et al., 1992, 1993) was that northern hemisphere summer insolation triggers a train of climatic responses that are initially transmitted via deep water to the southern hemisphere and only later drive northern hemisphere ice sheets via CO_2 changes and other feedbacks.

The decade since the SPECMAP effort ended has brought progress in several areas relevant to orbital-scale climate. Long ice-core records of greenhouse gases (including CO_2 and CH_4) have been recovered at the Vostok site in Antarctica (Petit et al., 1999). Recent work on the Vostok gas time scale (Shackleton, 2000; Ruddiman and Raymo, 2003) has brought the time control on ice-core gas signals to a level at least equal to that of the marine $\delta^{18}O$ signal.

Also, SPECMAP assumed that marine $\delta^{18}O$ signals are not seriously compromised by temperature overprints, but this assumption needs to be re-examined. Shackleton (2000) proposed that these overprints may be large enough to invalidate marine $\delta^{18}O$ as an ice-volume proxy.

Finally, independent techniques have converged on a marine $\delta^{18}O$ time scale that is older by 1500–2000 years than that of SPECMAP. These methods include: Th/U dating of early deglacial coral reefs (Edwards et al., 1987; Bard et al., 1990); tuning of the marine $\delta^{18}O$ record to insolation by relaxing the assumption of a constant phase lag (Pisias et al., 1990); and linking ice-core time scales to the marine $\delta^{18}O$ record (Shackleton, 2000; Ruddiman and Raymo, 2003).

These lines of progress motivated this review and synthesis of orbital-scale climatic changes. Section 1 summarizes the contrasting CLIMAP and SPECMAP views of orbital-scale climatic change. Section 2 summarizes progress in dating CO_2 and CH_4 changes in Vostok ice, and in revising the marine $\delta^{18}O$ time scale. Section 3 applies these findings to a critique of the SPECMAP models. Section 4 presents the approach used here to create a synthesis of orbital-scale climatic changes. Sections 5 and 6 summarize new syntheses of climatic responses to insolation forcing at the obliquity and precession periods. Section 7 presents a new hypothesis on the paced origin of the 100,000-year climate cycle. Section 8 applies these interpretations to changes observed during the last 10,000 years.

1. CLIMAP and SPECMAP: differing views of orbital climate changes

1.1. The CLIMAP model

1.1.1. Obliquity and precession

Hays et al. (1976a) first confirmed the Milankovitch (1941) hypothesis that northern hemisphere ice sheets are externally forced by summer-insolation changes. This forcing/response model was applied to the 41,000-year period of obliquity and the 23,000-year (and 19,000-year) period of precession (Figs. 1 and 2), but not to the 100 000-year eccentricity cycle. The critical mechanism in this model is control of ice ablation by insolation during warm summers.

Imbrie et al. (1984) used the marine $\delta^{18}O$ signal as an index of the timing of ice-volume change and tuned it to summer insolation with appropriate lags. Based on glaciological estimates (Weertman, 1964), the ice sheets were given a time constant of response of 17,000 years. Orbital obliquity (“tilt”) is the simplest period to analyze, because the forcing is a simple either/or choice; summer or winter. Imbrie et al. (1984) positioned the 41,000-year marine $\delta^{18}O$ signal 7900 years behind northern hemisphere obliquity forcing (Fig. 1, left).

Interpreting climatic change at the 23,000-year period of orbital precession is more difficult. Insolation changes at this cycle are again precisely known, but the progression of orbital positions implicit in the word “precession” opens up a range of possible insolation forcing for every season and month of the year. As a result, it is necessary to identify the key season and hemisphere through which any 23,000-year response observed on Earth is registered. Both CLIMAP and the early SPECMAP efforts used the June 21 summer solstice as a reference point for summer insolation (Fig. 2, left), but this choice was admitted to be an arbitrary one. The 23,000-year marine $\delta^{18}O$ signal lagged 5000 years behind June 21 insolation (Fig. 2, left).

1.1.2. Eccentricity

The 100,000-year component in marine $\delta^{18}O$ signals was interpreted differently. Even though external insolation forcing from changes in orbital eccentricity is negligible, the timing of the 100,000-year $\delta^{18}O$ response for some reason fell close to that of orbital eccentricity. As a result, Hays et al. (1976a) regarded this signal as a “paced”, rather than a forced, response. Use of the word “pacemaker” in their paper reflected this interpretation. These views of climatic change at the periods of obliquity, precession, and eccentricity

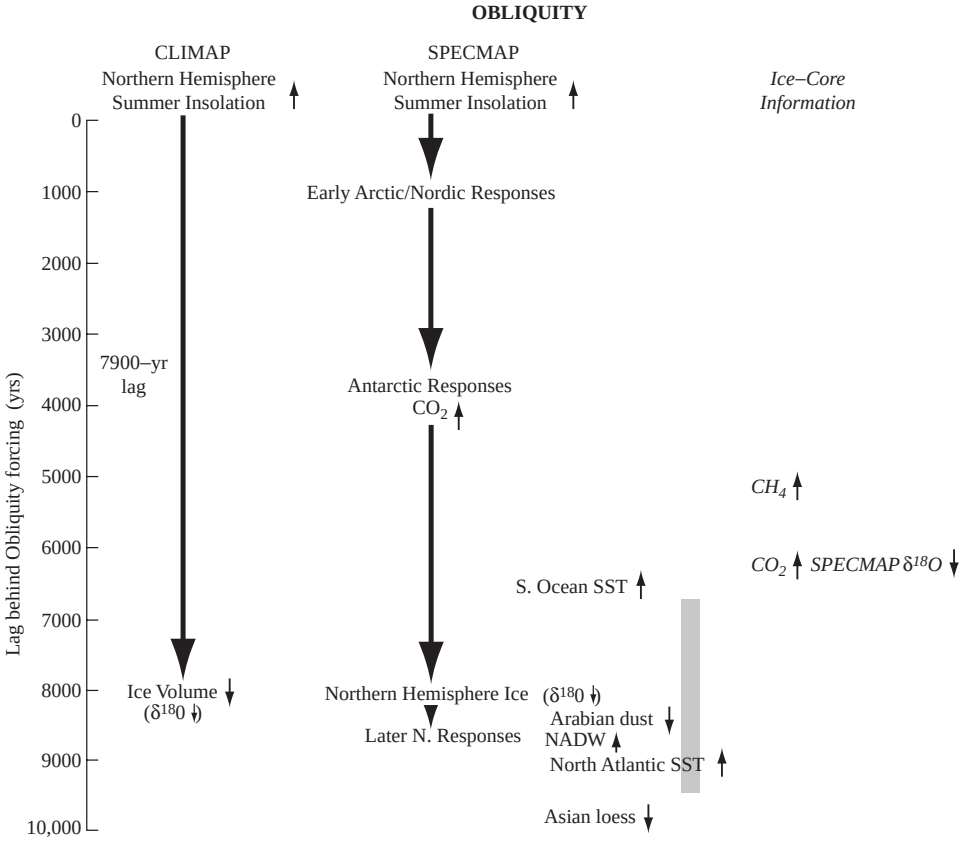

Fig. 1. (Left) The CLIMAP model proposed direct insolation forcing at the obliquity period, and this assumption was later used by Imbrie et al. (1984) to develop a tuned $\delta^{18}O$ time scale. (Center) The SPECMAP model proposed that summer insolation forcing causes energy propagation through a sequence of internal climate-system responses that drive northern ice sheets. (Right) New dating of Vostok gas signals and marine $\delta^{18}O$ records can be used to test the SPECMAP model. Small arrows indicate sense of response (increase or decrease) to increased summer insolation.

prevailed during the CLIMAP era (1976–1984) and are referred to here as the "CLIMAP Model".

In the late 1980s, however, a major revision of this view began within SPECMAP. One reason for this shift was the completion of an ambitious compilation of regional orbital-scale responses in ocean surface temperature, or SST (Imbrie et al., 1989). Compared to the marine $\delta^{18}O$ signal used as the timing reference, SST responses in the South Atlantic and Southern Ocean tended to occur early, while those in the North Atlantic tended to occur late. Similarities in phasing of the SST responses among the three orbital periods pointed to some kind of common sequence of cause and effect in the climate system. In addition, newly emerging carbon-isotopic ($\delta^{13}C$) and Cd/Ca data were being applied to try to reconstruct the timing of changes in atmospheric CO_2. At that time, however, published ice-core CO_2 records were still too short for spectral analysis.

1.2. The SPECMAP model

Imbrie et al. (1992, 1993) summarized a new model of orbital-scale climate change for all three orbital periods, here referred to collectively as the "SPECMAP Model".

1.2.1. Obliquity and precession

For obliquity and precession, SPECMAP continued to invoke northern hemisphere summer insolation as the initial source of forcing, although choosing June 1 rather than June 21 insolation as the critical time of year. But SPECMAP now proposed an entirely different mechanism of internal climate-system responses from those of CLIMAP.

The SPECMAP model proposed a train of responses by means of which initial northern summer insolation forcing was sequentially transmitted through the climate system and eventually to the ice sheets (Figs. 1 and 2, center). The first step in the sequence was a 1000-year delay in the response of Arctic ice and snow to insolation forcing. Next, a very early deep-water response was transmitted from the near-Arctic Nordic Sea to the Southern Ocean via changes in heat content of lower North Atlantic Deep Water. Once this signal arrived in the Southern Ocean, it caused a slow response in southern hemisphere sea ice, marine ice sheets, ocean circulation, and carbon storage. These changes caused variations in atmospheric CO_2. The proposed time constant of 3000 years for this complex of southern-hemisphere responses added phase lags of 2500–3000

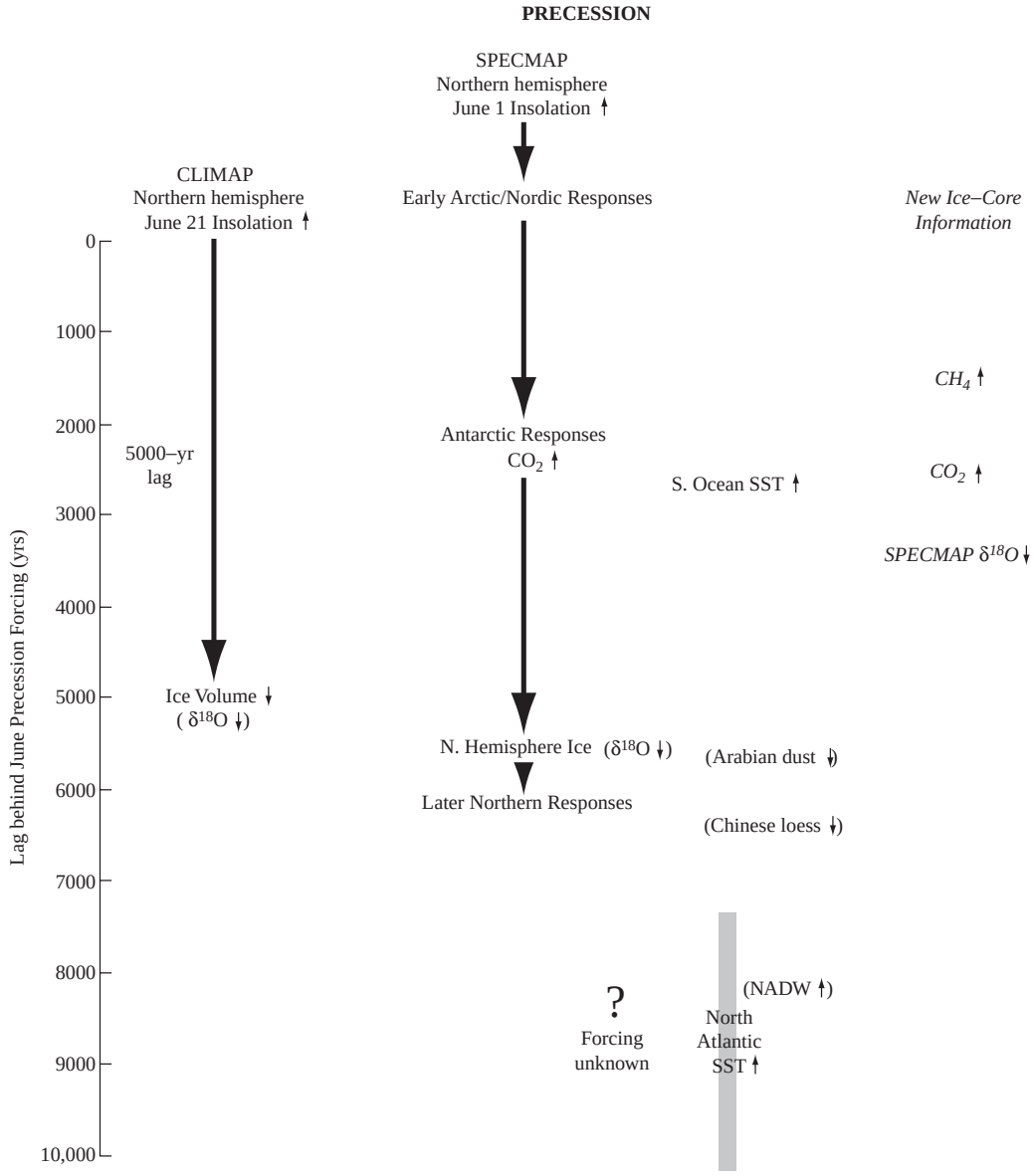

Fig. 2. (Left) The CLIMAP model proposed direct insolation forcing at the precession period, and this assumption was later used by Imbrie et al. (1984) to develop a tuned $\delta^{18}O$ time scale. (Center) The SPECMAP model proposed that June 1 insolation forcing causes energy propagation through a sequence of internal climate-system responses that drive northern ice sheets. (Right) New dating of Vostok gas signals and marine $\delta^{18}O$ records can be used to test the SPECMAP model. Small arrows indicate sense of response (increase or decrease) to increased summer insolation.

years to the cumulative propagation of energy through the climate system. The next step in this train of responses was the forcing of northern hemisphere ice sheets by the processes in the south, primarily by changes in atmospheric CO_2. The original CLIMAP time constant of northern ice response of 17,000 years was reduced to 5000 years (Imbrie et al., 1992). As a result, the ice sheets responded to CO_2 forcing with phase lags of 3400-4300 years (Figs. 1 and 2, center). Finally, the ice sheets forced proximal regional responses in high northern latitudes through the effects of their albedo and elevation with a delay of 500 years.

Although not widely understood, the SPECMAP model of climate-system behavior at the periods of obliquity and precession amounts to a total abandonment of the Milankovitch-based CLIMAP view. Instead of direct insolation forcing of northern ice, climatic changes were first registered in the Arctic, then transmitted into the southern hemisphere and finally sent back north to drive the ice sheets.

This claim can be substantiated by examining the SPECMAP sequence of responses in the light of the 5000-year ice-sheet time constant of the ice sheets. Imbrie et al. (1984) used an equation from Jenkins and Watts (1968) that links ice-sheet time constants with the

phase lags of the 41,000-year and 23,000-year $\delta^{18}O$ signals behind insolation forcing:

$$\phi = \arctan 2\pi fT,$$

where ϕ is the observed phase lag in degrees, f is the forcing frequency in years (1/41,000 or 1/23,000), and T is the time constant in years.

For a 5000-year ice time constant, ice volume (marine $\delta^{18}O$) should lag 4200 years behind the primary forcing at 41,000 years and 3400 years behind the primary forcing at 23,000 years. These are precisely the lags of the northern hemisphere ice sheets behind CO_2 in the SPECMAP model (Figs. 1 and 2, center). This match confirms that CO_2 is the direct source of forcing for northern hemisphere ice sheets, rather than the summer-insolation changes that produce the early "ice-sheet margin" response in the Arctic after a 1000-year "delay". In summary, the very early climatic response inferred by SPECMAP for the Arctic cannot be the main ice-sheet response. This confirms that the SPECMAP model abandoned this key feature of the Milankovitch mechanism.

1.2.2. Eccentricity

SPECMAP also devised a new hypothesis for the origin of the 100,000-year climate signal (Imbrie et al., 1993). Rather than being a paced response as in CLIMAP (Hays et al., 1976a), SPECMAP proposed that the 100,000-year ice-volume ($\delta^{18}O$) signal is a forced response. The logic behind this interpretation was the apparent similarity of the sequencing of many climate-system responses at the 100,000-year period to those at the forced responses of 41,000 and 23,000 years. This similarity implied that some kind of direct forcing must also lie behind the 100,000-year responses, even in the absence of obvious external forcing. SPECMAP inferred that a source internal to the climate system must exist and called it "internal thermal forcing".

SPECMAP also noted that a phase delay of 12,000 years or more existed between some of the earliest 100,000-year responses and the later marine $\delta^{18}O$ (ice-volume) response. This very long delay suggested that the 100,000-year ice sheets must respond to the proposed internal thermal forcing with a large time constant (15,000 years) as a result of their massive size.

In the SPECMAP model, the (unknown) "internal thermal forcing" at 100,000 years produces a train of climate-system responses analogous to those at 41,000 and 23,000 years (Fig. 3). These consist of: a 1000-year Arctic delay; subsequent transmission via deep-water flow to the Southern Hemisphere; a phase lag of just under 3000 years caused by the time constant of the southern-hemisphere responses; CO_2 forcing of northern ice sheets with a 12,000-year phase lag, and final transfer of the ice-sheet response to nearby northern regions.

SPECMAP (Imbrie et al., 1993) summarized evidence for similar sequences of regional responses at all three orbital periods based on SST evidence and on geochemical indices of nutrient redistribution in the ocean. The pattern of early Southern Ocean SST responses had first been defined by Hays et al. (1976a) in core RC11-120 at 44°S in the Indian Ocean. Late-phased responses at 41,000 and 100,000 years had also been detected in ice-proximal regions of the northern hemisphere and attributed to the effects of northern ice sheets by Ruddiman and McIntyre (1984). These responses included faunal estimates of North Atlantic SST, as well as $\delta^{13}C$-based estimates of North Atlantic Deep Water flow (Raymo et al., 1990) and depositional fluxes of Arabian dust (Clemens and Prell, 1990) and Asian loess (Kukla et al., 1990).

1.2.3. Model limitations

SPECMAP noted several vulnerable aspects in their model. The initial 1000-year delay in the circum-Arctic climatic response to summer insolation was inserted on a somewhat ad hoc basis. Such a delay was initially deemed necessary to avoid an unreasonably long time constant of ice-sheet response to insolation forcing. Using the equation of Jenkins and Watts (1968), Imbrie et al. (1992) calculated that the observed marine $\delta^{18}O$ (ice-volume) lags at 41,000 and 23,000 years would require unjustifiably long ice time constants of 37,000 and 70,000 years, close to the infinite time constant for a phase lag of 90°. As a result, a 1000-year delay was inserted to reduce the lags and produce more reasonable time constants for the ice sheets. (In a sense, however, this choice is odd, because the published SPECMAP model also abandoned direct insolation forcing of ice sheets, as noted above.)

A second issue was the paucity of evidence for a "very early" response at periods of precession and obliquity in long-term proxy signals of circum-Arctic climate and deep-water temperature. In support of the SPECMAP hypothesis, Imbrie et al. (1992) noted evidence of a late Holocene cooling in the Nordic Sea, but no longer-term orbital signal of this kind could be identified.

Another problem with the SPECMAP model was that it was incompatible with some observations. For example, Southern Ocean SST led marine $\delta^{18}O$ by only 1100–1800 years at the 41,000-year cycle (Imbrie et al., 1989), and this late phasing left inadequate time for the required 41,000-year response of northern ice sheets to forcing from the south. In addition, the cluster of late 23,000-year SST responses in North Atlantic cores from north of 40°N did not fit the SPECMAP model (Fig. 2, center). The SST phase lags versus $\delta^{18}O$ in these cores ranged from 700 to 3500 years and averaged 2700 years. These SST lags behind $\delta^{18}O$ were too large to be explained as proximal responses to the northern ice sheets, as had been the case for obliquity (Fig. 1, center).

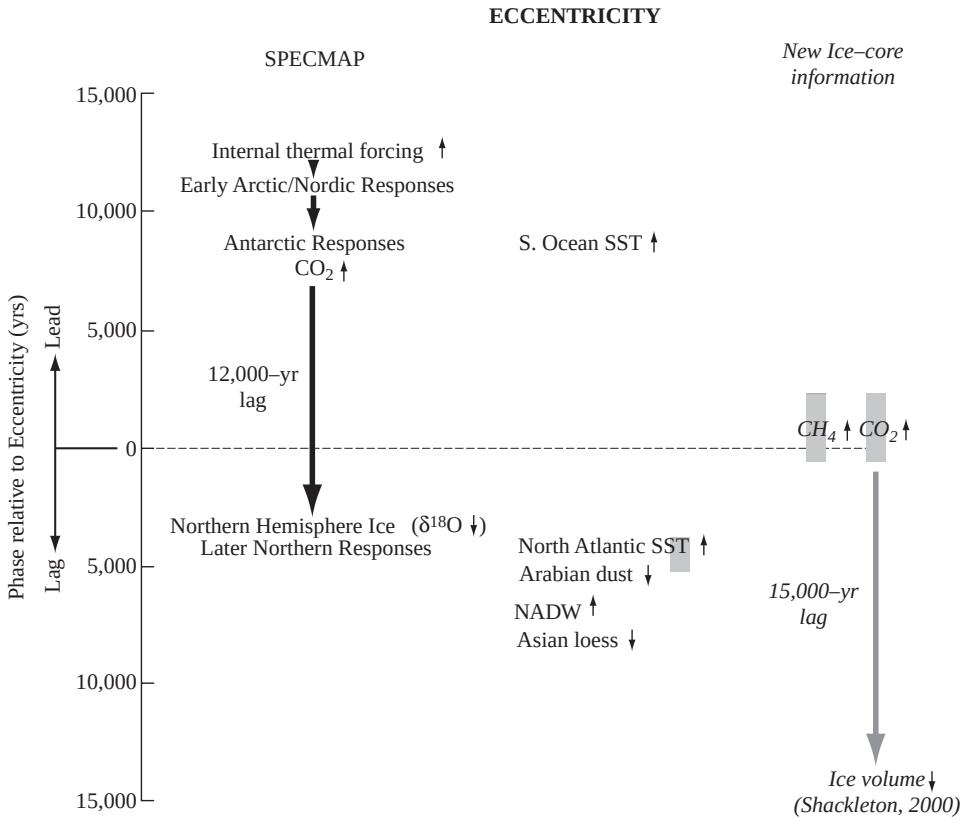

Fig. 3. In the CLIMAP view (not shown), northern hemisphere ice-sheet changes at the 100,000-year cycle are paced by eccentricity. (Left) In the SPECMAP model, the 100,000-year ice-volume signal is driven by internal forcing. (Right) New dating of Vostok gas signals and marine $\delta^{18}O$ records can be used to test the SPECMAP model. Shackleton (2000) found that CO_2 changes have a phase near eccentricity, and concluded that the ice-volume response lags CO_2 by 15,000 years. Small arrows indicate sense of change (increase or decrease) when eccentricity is high.

SPECMAP called these late responses "unexplained" (Imbrie et al., 1992).

A major omission from the SPECMAP model was any treatment of climatic processes in the tropics. Neither precessional insolation forcing of tropical monsoons (Kutzbach, 1981; Prell and Kutzbach, 1987) nor the possible impact of monsoon-generated CH_4 signals (Chappellaz et al., 1990) on other regions was included in the sequence of 23,000-year responses.

Finally, SPECMAP was unable to identify a credible early phased source for the proposed internal thermal forcing at 100,000 years. Imbrie et al. (1993) noted that the first derivative of sea level had the appropriate phase and proposed that the vulnerability of marine ice sheets to early sea-level rise at the 100,000-year cycle might play a role in this internal forcing. But SPECMAP also admitted that this explanation would only work for the large ice sheets at the 100,000-year cycle, and only on deglaciation, but not on ice growth.

2. Orbital records of greenhouse gases from Vostok ice

In the decade after SPECMAP ended, the completion of drilling at Vostok produced valuable records of climatic indices extending back 400,000 years. The long-term CO_2 and CH_4 records, along with other constituents, provide an obvious potential for improving knowledge of key interactions within the climate system, provided that they can be dated with sufficient accuracy.

Dating of the upper part of the Vostok ice-core record has a long history summarized by Jouzel et al. (1993). Following completion of deep drilling, Petit et al. (1999) published multiple ice-core signals based on the GT4 time scale for levels prior to 200,000 years BP. The estimated age uncertainty for the GT4 time scale was about 5%, ranging from ± 5000 years for ice younger than 100,000 years to $\pm 15{,}000$ years for ice older than 300,000 years BP.

Shackleton (2000) proposed a time scale for Vostok ice (here called the $\delta^{18}O_{atm}$ time scale) based on tuning $\delta^{18}O_{atm}$ (the $\delta^{18}O$ value of air trapped in the ice) to an orbital insolation signal comprised of tilt and precession. Bender et al. (1994) had shown that the $\delta^{18}O_{atm}$ signal is influenced both by ice sheets (because the mean $\delta^{18}O$ value of sea water affects the $\delta^{18}O_{atm}$ of air, with a lag of about 1000 years) and by tropical monsoons (because of changes in global-mean photosynthetic activity). Shackleton assumed that the phase of $\delta^{18}O_{atm}$

is determined by two factors: the lag of ice sheets behind insolation forcing, and the phase of tropical monsoons relative to precession insolation forcing. He selected a constant phase lag of $\delta^{18}O_{atm}$ behind insolation that he judged would satisfy both of these assumed controls.

Ruddiman and Raymo (2003) devised a "CH_4 time scale" for Vostok ice by tuning CH_4 (gas) to insolation at 30°N. This effort was based on the orbital monsoon hypothesis of Kutzbach (1981), in which summer insolation maxima at the precessional rhythm in north-tropical latitudes heat the land and pull in moist ocean air, creating monsoons. The timing was based on the most recent CH_4 maximum in annually layered GRIP ice (Blunier et al., 1995), which had the same phase as mid-July insolation. The CH_4 time scale matched those of Petit et al. (1999) and Shackleton (2000) to within about 5000 years back to 200,000 years ago. Prior to 200,000 years ago, the $\delta^{18}O_{atm}$ and CH_4 time scales diverged considerably from the GT4 time scale of Petit et al. (1999), but remained relatively similar to each other. In this earlier interval, the GT4 time scale at times requires an unlikely out-of-phase relationship of CH_4 and insolation. On average, the CH_4 and $\delta^{18}O_{atm}$ time scales are offset by only 450 years. This convergence indicates significant progress in obtaining a reliable time scale for Vostok ice. The CH_4 time scale is used in this paper.

For Vostok CH_4 and July 30°N insolation, the 23,000-year precession signal is dominant (Fig. 4). The amplitudes of CH_4 maxima are modulated by insolation, but CH_4 minima show little if any modulation. The CH_4 spectral peak at 100,000 years is largely caused by truncation of 23,000-year CH_4 minima, leaving CH_4 maxima unbalanced by comparable CH_4 minima. A weak signal is also present at the 41,000-year period of orbital obliquity. The origin and phasing of the CH_4 signals at obliquity and eccentricity will be discussed in Sections 5 and 7.

The CH_4 time scale can be used to examine CO_2 variations in Vostok air samples. The CO_2 signal is similar to the marine $\delta^{18}O$ record (Fig. 5), as noted by Genthon et al. (1987). The two signals are highly coherent (correlated) at all three orbital periods, with CO_2 leading $\delta^{18}O$ by 2300 years at the 23,000-year precession period, 1400 years at the 41,000-year obliquity period, and 6600 years at the 100,000-year eccentricity period. For both obliquity and precession, the phasing of CO_2 versus $\delta^{18}O$ in the $\delta^{18}O_{atm}$ time scale is nearly identical (to within 100 years) to that of the CH_4 time scale, a further indication of their close convergence.

Several lines of evidence indicate that the $\delta^{18}O$ time scale of Imbrie et al. (1984) should be revised toward older ages. Dating of coral reefs (Edwards et al., 1987; Bard et al., 1990) has shown evidence of fast deglaciation to the high stands of sea level representing ice-volume (and $\delta^{18}O$) minima. In addition, Pisias et al. (1990) allowed for variations in the phase of the precession and obliquity $\delta^{18}O$ signals (and presumed ice-volume responses) to orbital forcing and found a mean 1500-year offset of the SPECMAP $\delta^{18}O$ signal toward older ages. Shackleton (2000) re-tuned the marine $\delta^{18}O$ time scale using shorter phase lags of $\delta^{18}O$ behind insolation than those of Imbrie et al. (1984). His revision of the marine $\delta^{18}O$ time scale was offset an average of 2000 years older than SPECMAP. The 1500-year mean offset of Pisias et al. (1990) is consistent with the CH_4 time scale of Ruddiman and Raymo (2003) used here.

If the SPECMAP $\delta^{18}O$ signal is moved back 1500 years relative to the time scale in Imbrie et al. (1984), the CO_2 leads relative to the marine $\delta^{18}O$ signal in Fig. 5 are reduced accordingly. This revision also reduces the lags of the $\delta^{18}O$ signals behind summer insolation at all three orbital periods. The adjusted marine $\delta^{18}O$ phases are plotted to the right in Figs. 1 and 2. The 7900-year lag of the 41,000-year $\delta^{18}O$ signal behind summer insolation is reduced to 6400 (hereafter 6500) years (Fig. 1, right), and the 5000-year lag of the 23,000-year signal behind June 21 insolation is reduced to 3500 years (Fig. 2, right). Although not shown, the phases of all other climatic responses determined relative to the marine $\delta^{18}O$ record also shift by 1500 years.

Also plotted on the right in Figs. 1–3 are the phases of the CO_2 and CH_4 signals determined from Vostok ice by Ruddiman and Raymo (2003). At the obliquity period, the 41,000-year CH_4 signal leads SPECMAP $\delta^{18}O$ by 1800 years, while the CO_2 signal is in phase with SPECMAP $\delta^{18}O$ to within 100 years (Fig. 1, right). For precession, the 23,000-year CH_4 signal in Vostok ice lags June 21 insolation by 1500 years (because it was tuned to mid-July insolation), and the 23,000-year CO_2 signal leads the SPECMAP $\delta^{18}O$ signal by 800 years (Fig. 2, right). At the 100,000-year cycle, the phase of the orbital eccentricity signal is a useful reference point for comparing the relative timing of other climatic changes. After the 1500-year time-scale adjustment, the marine $\delta^{18}O$ signal lags eccentricity by 1800 years, while CO_2 leads it by 3300 years or less and CH_4 leads by 1600 years.

Shackleton (2000) found that the observed phase of the 100,000-year benthic $\delta^{18}O$ signal in an eastern Pacific core could be an artifact derived from combining a deep-water temperature signal phased several thousand years ahead of eccentricity with an ice-volume signal phased far behind it. His interpretation placed the phase of the 100,000-year ice-volume response much later than that of the SPECMAP model (Fig. 3, right). Although this large a delay in ice-volume phasing will be examined and rejected in Section 3, Shackleton's paper highlights an important complication

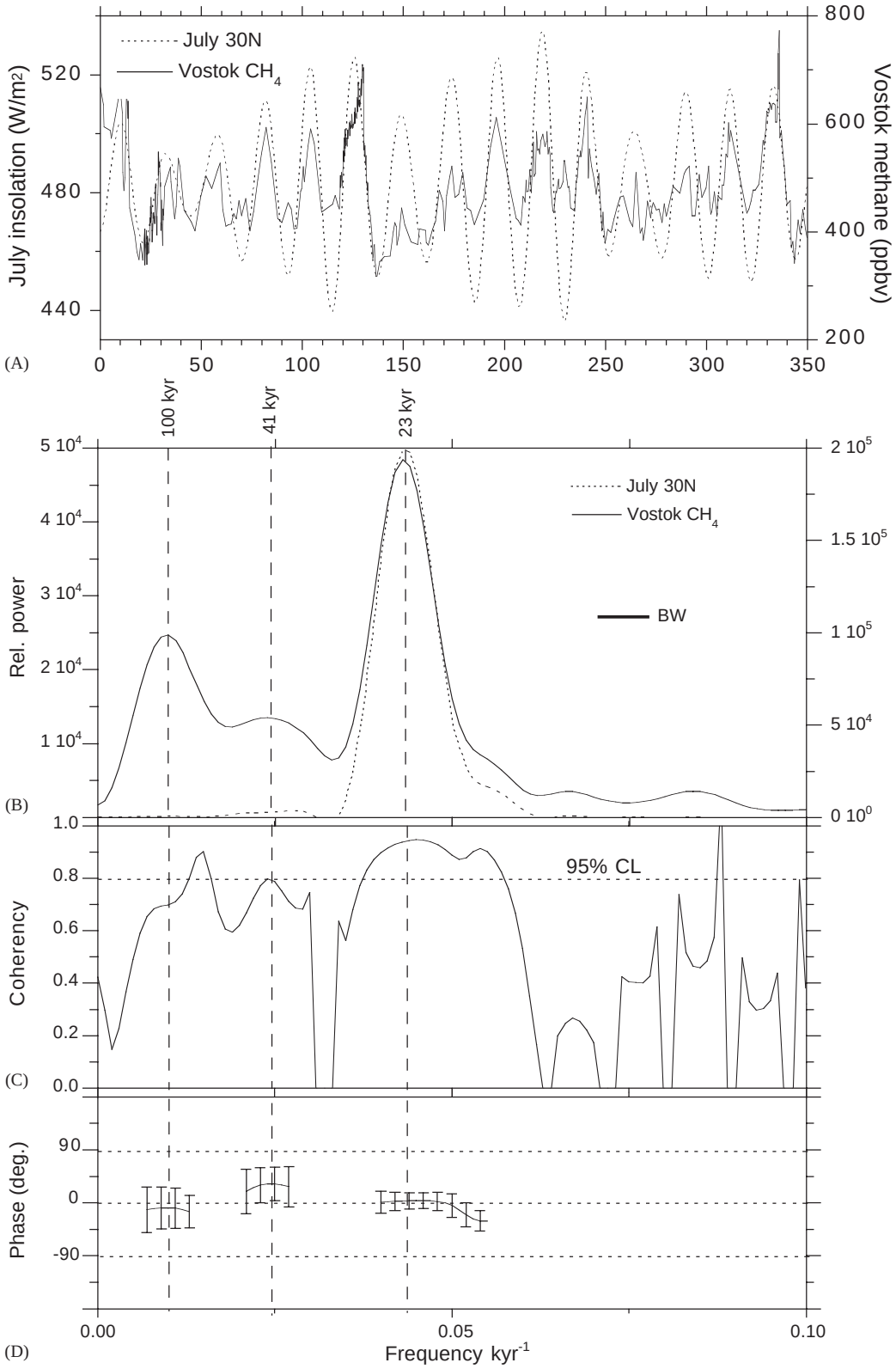

Fig. 4. Comparison of Vostok CH_4 (plotted on the CH_4 time scale of Ruddiman and Raymo, 2003) and July 30°N insolation. (a) Time series. (b–d) Cross-spectral analysis: (b) power spectra; (c) coherence between CH_4 and insolation; and (d) phasing at orbital periods, with 95% confidence intervals indicated. Spectral analysis base on Blackman–Tukey method, with $\frac{1}{3}$ lags.

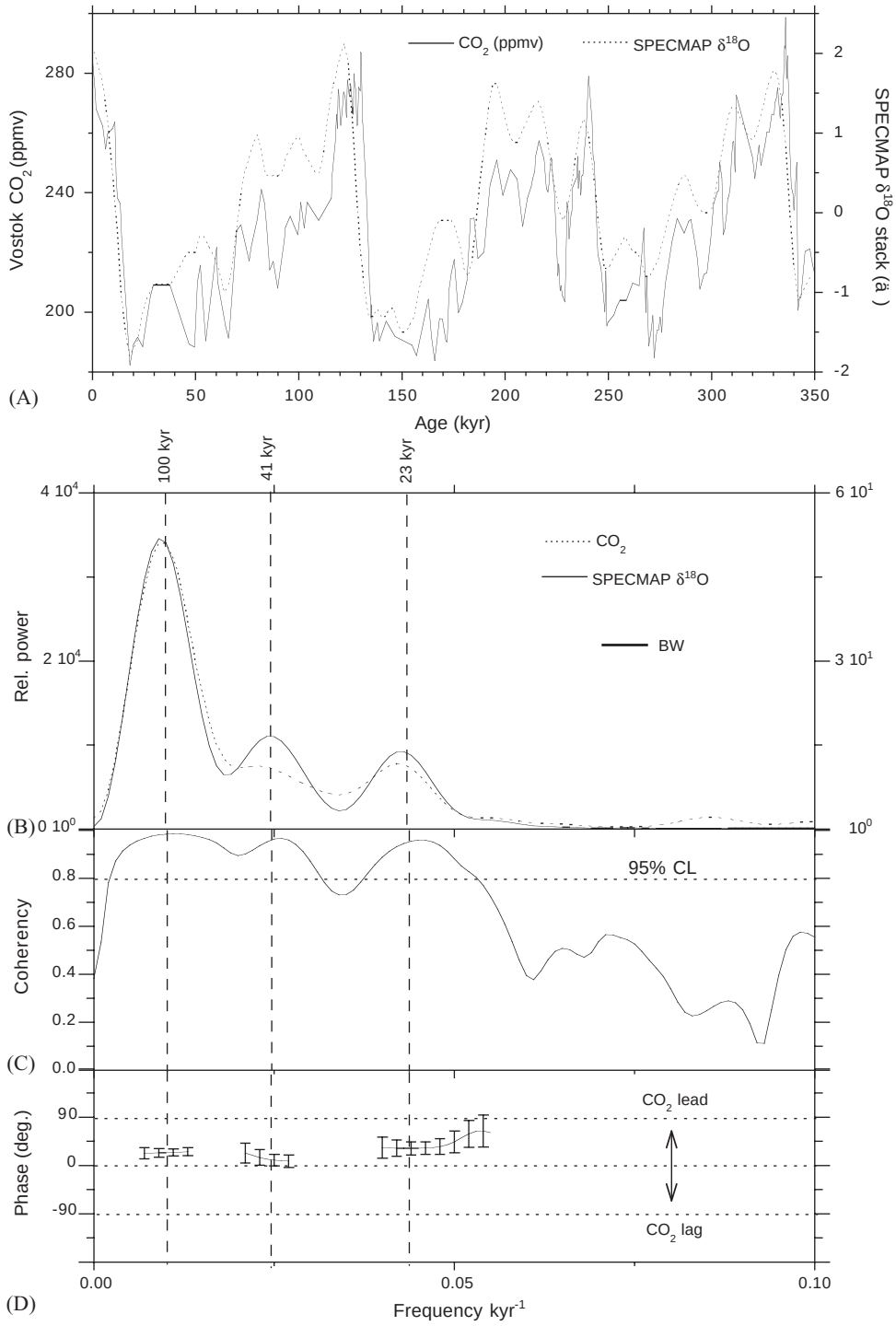

Fig. 5. Comparison of Vostok CO_2 (plotted on the CH_4 time scale of Ruddiman and Raymo, 2003) and the $\delta^{18}O$ time scale of Imbrie et al. (1984). (a) Time series. (b–d) Cross-spectral analysis: (b) power spectra; (c) coherency between CO_2 and $\delta^{18}O$ signals; and (d) phasing at orbital periods, with 95% confidence intervals indicated. Spectral analysis based on Blackman–Tukey method, with $\frac{1}{3}$ lags.

not considered by SPECMAP: marine $\delta^{18}O$ signals may be a poor indicator of the true phase of orbital-scale ice-volume changes because of temperature overprints. The approach outlined in Section 4 makes use of this insight in devising a new synthesis of climate change.

3. The SPECMAP model: an updated critique

The first part of this section uses the newly dated orbital-scale CO_2 and CH_4 signals and the 1500-year shift of the marine $\delta^{18}O$ time scale to test the SPECMAP model of orbital climate change. The last part is an

evaluation of the SPECMAP analysis of the 100,000-year cycle.

3.1. Testing the SPECMAP model against new information

As noted above, the shift of the $\delta^{18}O$ time scale of Imbrie et al. (1984) toward older ages reduces the lag of $\delta^{18}O$ behind insolation forcing at the obliquity and precession periods in the CLIMAP model. This relative shift in turn reduces the time constant of ice-sheet response (a point to be explored further in Sections 5 and 6). In the SPECMAP model, this age shift would eliminate any need to invoke an initial 1000-year delay tied to Arctic/Nordic climatic responses in order to avoid unreasonably large ice time constants.

The availability of ice-core gas signals with well-constrained timing also permits a more diagnostic test of the SPECMAP model. A key feature of that model was the shift of carbon and nutrient proxies among deep-ocean reservoirs. SPECMAP inferred that changes in these proxies revealed the timing of changes in atmospheric CO_2. For all three orbital periods, SPECMAP positioned the changes in carbon distribution in the "early" group of southern-hemisphere responses that included sea ice and marine ice sheets. These southern-hemisphere responses preceded and were assumed to drive changes in northern hemisphere ice volume.

Both during and since the SPECMAP era, interpreting geochemical indices of nutrients and carbon became more complex as complicating factors emerged (for example, Boyle, 1992). These indices often disagree about the amount and even the sign of carbon-system and nutrient changes, and the disagreements have been greatest in the Southern Ocean region. Even now, the causal links between shifts of carbon and nutrients in the ocean and changes in atmospheric CO_2 remain illusive. Fortunately, with long records from Vostok now available, it is possible to bypass these complications and use the ice-core CO_2 record directly to test the SPECMAP model. The critical question is this: Does the CO_2 signal fall on or near the phase proposed by SPECMAP?

For the orbital obliquity period of 41,000 years, the answer is no. The CO_2 signal has a phase identical to that of marine $\delta^{18}O$, rather than leading it by some 4350 years, as in the SPECMAP model (Fig. 1). This identical phasing of CO_2 and $\delta^{18}O$ is incompatible with the train of responses proposed by SPECMAP. If $\delta^{18}O$ is an index of ice volume, this very similar phasing rules out the possibility that an early CO_2 response forces a later ice-volume response.

For the 23,000-year precession period, the CO_2 signal has the same early phase as the southern-hemisphere responses, consistent with SPECMAP (Fig. 2). But now the later part of the train of 23,000-year responses has become inconsistent with the SPECMAP model. With the marine $\delta^{18}O$ signal adjusted by 1500 years, the lead of the CO_2 signal relative to $\delta^{18}O$ is reduced to 800 years, much less than the 3400-year lead at the precession cycle required for an ice-sheet time constant of 5000 years. While these new phase relationships do not rule out some kind of "causal" role for the early 23,000-year CO_2 signal, the full sequence does not fit the SPECMAP model.

For the orbital period of 100,000 years, the phase of the CO_2 signal inferred from ice cores is far different from the SPECMAP model (Fig. 3). Rather than leading the 100,000-year marine $\delta^{18}O$ signal by 12,000 years, CO_2 has a phase close to that of eccentricity and a lead of no more than 5000 years ahead of marine $\delta^{18}O$. A lead that small is incompatible with the SPECMAP model of massive 100,000-year ice sheets with a 15,000-year time constant (Imbrie et al., 1993).

In summary, the phasing of CO_2 at all three orbital periods disagrees in one respect or another with the train of responses predicted by the SPECMAP model. This does not invalidate the phases of deep-water flow and nutrient/carbon redistribution cited by SPECMAP. Still, if these proxy indices do not define the timing of atmospheric CO_2 changes, they apparently are not part of the central causal pathway in the climate system. Not all climate-system responses need be in the critical train of causal linkages; some may simply be "side tracks off the main line". The above analysis also challenges the central SPECMAP assumption that analogous trains of energy move through the climate system in a similar manner at all three orbital periods. Instead, the differences among the responses at the three orbital periods appear at least as noteworthy as the similarities.

3.2. Problem #1 with 100 K cycles: Rectification can shift their phase

The 100,000-year cycle can take two basic shapes. One is the "square-wave" shape that distinguishes colder conditions in glacial Isotopic Stages such as 2–4, 6, and 8 from generally warmer conditions in interglacial Stages such as 1, 5, 7, and 9. The basic sense of a square wave is that climate tends to be either glacial or interglacial, but not often in between. This shape was the reason for originally defining and numbering the younger isotopic stages. The other basic shape is the "saw-toothed" form produced by very rapid deglacial transitions (terminations) from full-glacial to full-interglacial conditions within 10% of each 100,000-year cycle, followed by much more gradual returns to full-glacial conditions over the other 90% of the cycle. Most climatic signals are a combination of the asymmetric saw-toothed shape and the more symmetric square-wave shape.

A major problem in interpreting some 100,000-year climatic responses is that they are "rectified" or "clipped", that is, truncated on one side or the other of their full range of response. SPECMAP did not address rectification, but this truncation can distort the phase of 100,000-year cycles detected by spectral analysis.

Two kinds of rectification are common. One is caused by the climate system. For example, oceans at high latitudes have a naturally limited response to forcing toward colder SST's because they reach the point at which seawater freezes and no further cooling can occur. The second kind of rectification arises from limitations in the proxy recorders of climate. Most such cases occur near the cold extreme of the range of response. Southern Ocean radiolarian assemblages cannot be used to estimate winter SST values colder than 4°C, because that is the modern-day limit beyond which the assemblages no longer vary in response to even colder conditions (Hays et al., 1976b). The same problem recurs for North Atlantic planktic foraminifera for winter SST values below 0°C (very near the freezing point of seawater).

An example of how rectification can alter the phase of climatic responses is shown in Fig. 6. The "generic" climate signal shown has aspects of both the saw-toothed and square-wave shapes and is similar to the last two 100,000-year signals in the $\delta^{18}O$ and CO_2 records (Fig. 5). For the full signal, the eye can easily see the 100,000-year cycle extracted by filtering (Fig. 6, top).

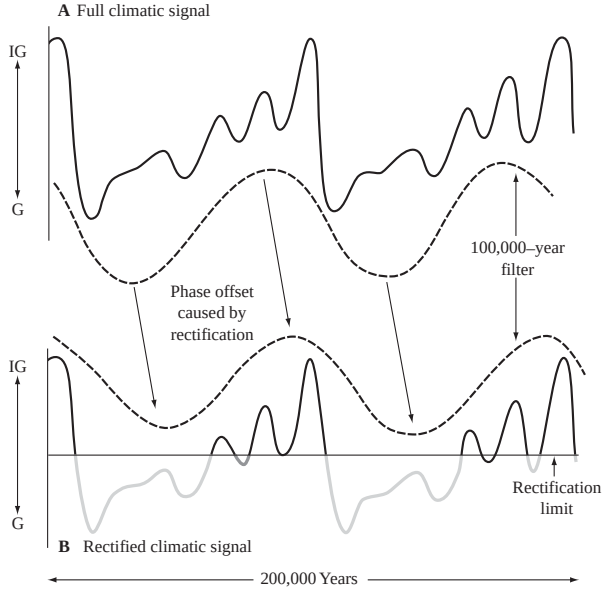

Fig. 6. (Top) If a climatic signal with a saw-toothed shape is fully expressed by a proxy indicator, a 100,000-year filter will extract the 100,000-year phase shown. (Bottom) But if the same climatic signal is rectified (truncated) at its cold extreme, a 100,000-year filter will be drawn toward the warm climatic extremes of the original signal, creating an artificial phase lead.

But if this same signal is rectified on the cold side of its response, a 100,000-year filter will tend to ignore the now-structureless cold (glacial) parts of the record and be drawn toward the early interglacial warm peaks. As a result, the filter will now extract a 100,000-year signal with an earlier phase (Fig. 6, bottom). The greater the rectification of the signal, the earlier the apparent phase will be. The opposite case—warm-side rectification of a signal causing a shift of the filtered 100,000-year cycle toward later phases—is also possible.

This analysis shows that the phases of all 100,000-year signals plotted in Fig. 3 need to be re-examined for possible artifacts of rectification. The largest impacts are on the phase of 100,000-year SST signals, some of which were critical parts of the SPECMAP train of responses (Fig. 3). The following discussion references SST phases both to marine $\delta^{18}O$ and to eccentricity.

Core RC11-120 in the Southern Ocean was used by SPECMAP as the definitive example of an "early" southern SST response because of its 12,500-year SST lead versus $\delta^{18}O$, but this SST signal is strongly rectified at the 4°C radiolarian detection limit. Because cold-side rectification produces artificial leads (Fig. 6), this early phase is unreliable. SST phases in the remaining Southern Ocean cores range from smaller leads to slight lags with respect to eccentricity (Fig. 7).

Tropical Atlantic cores show variable 100,000-year SST phases versus $\delta^{18}O$ ranging from a lead of 10,200 years to a lag of 4000 years (Imbrie et al., 1989). All three SST signals are strongly dominated by a 23,000-year cycle with the same phase. The unexpectedly large phase differences at 100,000 years appear to be the result of subtle differences in the amplitudes of individual minima and maxima in the precession signal, perhaps tied to small non-linearities produced by the way the biota records surface-ocean changes. Within these large

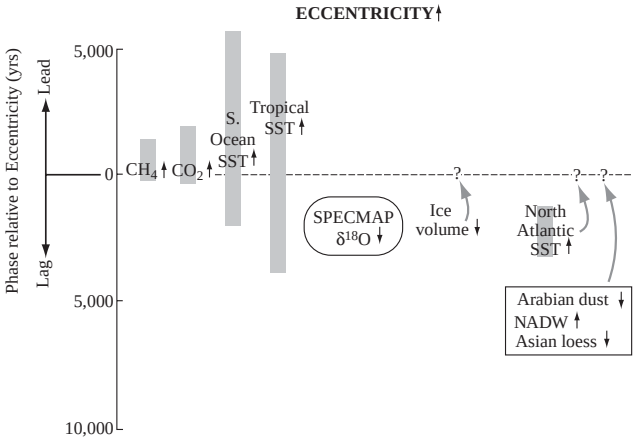

Fig. 7. After deletion of 100,000-year responses that are strongly rectified, the phases of the remaining 100,000-year climatic responses fall close to that of eccentricity. Small arrows indicate sense of change (increase or decrease) when eccentricity is high.

uncertainties, the phase of the 100,000-year tropical SST signal could be identical with that of eccentricity.

In the North Atlantic Ocean, four cores from north of 40°N have SST phases relative to $\delta^{18}O$ ranging from a 13,000-year lead to a 3600-year lag (Imbrie et al., 1989). The two cores north of 55° are seriously rectified on the cold extreme by the foraminiferal detection limit noted earlier, and their early phases are rejected as artifacts of rectification. Of the remaining cores, the SST signal in one is not rectified and in the other is only slightly truncated at the cold extreme. These 100,000-year SST signals lag eccentricity by 2200–2800 years (Fig. 7).

Among the northern hemisphere signals interpreted as driven by ice-volume changes, both the Arabian dust signal (Clemens and Prell, 1990) and the Asian loess signal (Kukla et al., 1990) are rectified during warm climates, with low values persisting through all of interglacial Isotopic Stage 5. Similarly, the NADW signal used by SPECMAP (Raymo et al., 1990) is rectified at the interglacial extreme because cores near NADW sources register larger and more persistent NADW influences than those farther south in the path of flow. Given these rectifications, the true 100,000-year phase of these signals must be earlier than observed and closer to the phase of marine $\delta^{18}O$ and eccentricity (Fig. 7), although their exact phasing remains unknown.

The CH_4 signal is clearly rectified during CH_4 minima (Fig. 4), but in this case no major phase shift occurs because the CH_4 maxima still retain the phase of eccentricity modulation. The CO_2 signal in Fig. 5 does not appear to be rectified to any obvious extent.

With the most obvious artifacts of rectification discounted, the phases of all major 100,000-year signals converge on that of eccentricity (Fig. 7). Rejection of the very early 100,000-year response in Southern Ocean SST eliminates one of SPECMAP's key lines of evidence for the propagation of a train of 100,000-year responses through the climate system. Within the remaining phase uncertainties shown in Fig. 7, the SST responses in the Southern Ocean, the tropics, and the North Atlantic could all have identical phases. The remaining phase differences shown may well be artifacts of smaller rectification effects not yet addressed.

This tight clustering of phases also brings into question the forcing-and-response model proposed by SPECMAP for the 100,000-year cycle (Imbrie et al., 1993). In the SPECMAP model, the phase of CO_2 was placed among the very early responses, 8000 years ahead of eccentricity and 12,000 years ahead of ice volume (marine $\delta^{18}O$). CO_2 was assumed to be the major source of forcing for ice volume. But with CO_2 phased no more than 5000 years ahead of marine $\delta^{18}O$, the difference in timing no longer allows the "sluggish" response of massive 100,000-year ice sheets inferred by SPECMAP. Indeed, the tight clustering of phases brings into question the need for any forcing and response tied to the 100,000-year cycle in the sense proposed by SPECMAP.

3.3. Problem #2 with 100 K cycle: Spectral analysis cannot handle saw-toothed signals

Up to this point, the phase of the 100,000-year ice-volume signal has not been re-evaluated. Until recently, spectral analyses of orbital-scale climate had assumed that the 100,000-year phase of ice volume matches that of $\delta^{18}O$, although part of the $\delta^{18}O$ amplitude was acknowledged to result from temperature changes. As noted earlier, however, Shackleton (2000) inferred that about half of a deep-Pacific 100,000-year $\delta^{18}O$ signal was caused by temperature changes and that the true phase of ice volume lagged far behind both eccentricity and marine $\delta^{18}O$.

When compared to actual ice-volume trends during the last two deglaciations, however, this large a lag behind eccentricity is not credible. During the most recent deglaciation, eccentricity reached a maximum 13,500 years ago. A 15,000-year ice-volume lag would require a minimum in the 100,000-year ice-volume signal some 1500 years in the future, but this conclusion contradicts long-accepted evidence (summarized in Mix et al., 2001) that ice volume reached a minimum by 6000 years ago. Where are the large, sluggish 100,000-year ice sheets that should have been melting over the last 6000 years and that should still be melting today? They do not exist.

This kind of mismatch is even worse in Stage 5, where the phasing indicated by Shackleton (2000) predicts that the eccentricity maximum 113,000 years ago should be followed by a 100,000-year ice-volume minimum near 98,000 years ago. This conclusion is directly contradicted by coral-reef evidence: the smallest volume of global ice in Stage 5 occurred near 125,000 years ago, far ahead of the predicted minimum. Again, what is the location of these massive 100,000-year ice sheets that slowly melted between 125,000 and 98,000 years ago, and how did they manage to do so while insolation trends at the cycles of obliquity and precession fell and rose by large amounts?

These mismatches cannot have been masked by the superposition of opposing trends in ice volume at obliquity and precession. In Shackleton's analysis, the 100,000-year ice-volume cycle explains 40% of the orbital-scale ice-volume total, far too much for it to be hidden underneath the other trends. The 15,000-year lag of the 100,000-year ice-volume signal behind eccentricity proposed by Shackleton (2000) makes no sense based on reliable evidence and must be rejected.

In fact, this problem with the phase of the 100,000-year ice-volume signal is even more perplexing. If the phase of the 100,000-year $\delta^{18}O$ signal in Isotopic Stage 5 were shifted 15,000 years earlier to match that of

eccentricity, the $\delta^{18}O$ and ice-volume minima would then occur 113,000 years ago, but still 12,000 years after the Stage 5.5 sea-level maximum and ice-volume minimum. This timing would place the 100,000-year ice-volume minimum in the middle of an interval of low northern summer insolation at both the obliquity and precession cycles, and very near the time when the $\delta^{18}O$ signal was nearing the ice-volume maximum of Stage 5.4. Clearly, this kind of analysis of the 100,000-year ice-volume cycle has arrived at a "dead end": no plausible phasing of the marine $\delta^{18}O$ signal with respect to eccentricity (that is, any lag within a range from 0 to 15,000 years) can be reconciled with the known sea-level and ice-volume trends in Stage 5. What is the flaw in this analysis?

Part of the key to resolving this problem is tied to what Raymo (1997) called the "quantum" nature of terminations. Each broad eccentricity maximum at the 100,000-year cycle spans 2 or 3 individual insolation maxima at the precessional cycle. During the last several deglaciations, the climate-system response has latched onto one or the other of these precession maxima in creating the observed termination. As a result, all terminations occur at or very near even multiples of 4 or 5 precession cycles (90,000–115,000 years). The specific precession maximum chosen by the climate system depends on several factors. Most critical among these is close alignment with a nearby obliquity maximum. Modulation of precession by the longer-term 400,000-year eccentricity cycle also plays a role: it makes all precessional maxima in a particular 100,000-year cycle either weaker or stronger, thereby affecting which of the several peaks is chosen for the termination.

The deglaciation at Termination I occurred on a weak precession maximum and almost in phase with eccentricity because of close alignment of a modest precession peak with an obliquity maximum. In contrast, the Termination II deglaciation occurred some 17,000 years ahead of the eccentricity maximum, in part because of good alignment of precessional insolation with obliquity, but also because eccentricity modulation produced a strong precession maximum well before the eccentricity peak. At Termination III, the even stronger 400,000-year modulation of precession failed to produce a complete deglaciation because of relatively poor alignment between obliquity and precession. The implication of this "quantum" nature of terminations is that the start of interglaciations can vary widely with respect to eccentricity, sometimes occurring nearly in phase (Termination I) but sometimes leading eccentricity by 17,000 years or more (Termination II).

This highly irregular spacing of terminations with respect to eccentricity is important because terminations represent the beginning of the interglacial half of the "square-wave" 100,000-year cycles extracted by spectral analysis. In effect, a significant part of the phase of individual 100,000-year $\delta^{18}O$ cycles is determined by this somewhat erratic "quantum" choice of one particular precession maximum over another. The larger implication is that the measured 100,000-year phase of any signal that contains strong terminations (such as marine $\delta^{18}O$) is a highly smoothed average of an erratic phasing that actually varies considerably from cycle to cycle.

The second (and more fundamental) answer to the problem raised above is that the smooth form of *any* 100,000-year filter is doomed to misrepresent some aspect of any climatic signal that contains both the square-wave and saw-tooth shapes (Fig. 8). If the filtered 100,000-year $\delta^{18}O$ signal succeeds in capturing the square-wave (glacial/interglacial) form that defines the marine isotopic stages, it will under-represent the amount of ice present at the early interglacial minimum (Fig. 8, top). But aligning the filtered 100,000-year signal on (or closer to) the early interglacial ice-volume minimum will not solve the problem (Fig. 8, bottom). In this case, the smooth form of the filtered 100,000-year $\delta^{18}O$ signal requires significant ice melting prior to the termination, but actual $\delta^{18}O$ signals (and other climatic records) instead show that maximum ice volume was reached at that time. The unavoidable conclusion is that filtering saw-toothed marine $\delta^{18}O$ signals to extract a 100,000-year cycle will misrepresent independently known observations.

In summary, major, seemingly fatal, flaws have been identified in the SPECMAP models of climate change at all three orbital periods (Imbrie et al., 1992, 1993). The task ahead is to devise a new synthesis that matches all

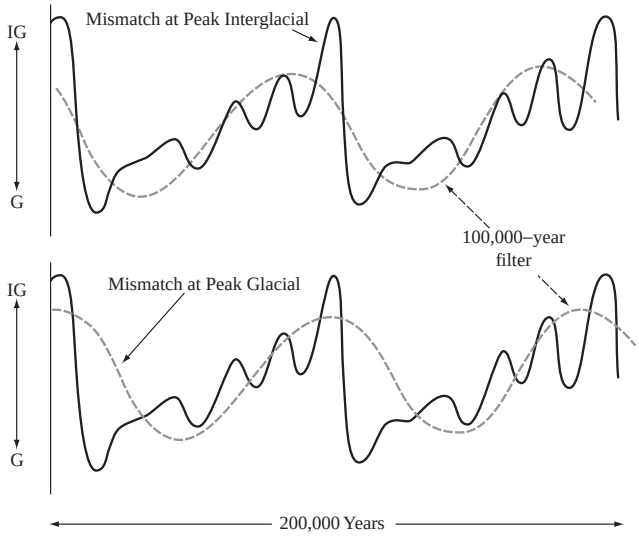

Fig. 8. A 100,000-year filter cannot capture the full form of climatic signals containing both saw-toothed and square-wave shapes. (Top) Filtered signals centered on the square-wave structure of marine isotopic stages seriously under-represent early interglacial ice-volume minima. (Bottom) Filtered signals centered on peak interglacial levels predict far too much deglaciation prior to terminations.

pertinent climatic observations and addresses the criticisms raised.

4. Analytical approach: toward a new orbital-scale climatic synthesis

4.1. The forced responses: obliquity and precession

The approach used here begins by reactivating the Milankovitch hypothesis that insolation directly forces northern hemisphere ice sheets at the periods of obliquity and precession. This hypothesis formed the centerpiece of the CLIMAP model, and Imbrie et al. (1984) used this physical link as the justification for tuning the marine $\delta^{18}O$ record to insolation. The hypothesis also has a solid physical basis: summer ablation of ice is a much stronger control of ice mass balance than accumulation of snow in winter (Oerlemans, 1991).

As in the SPECMAP project (Imbrie et al., 1992, 1993), the approach used here incorporates all major proxy indices of the behavior of the climate system: insolation, ice sheets, greenhouse gases and other regional responses. The approach used here also goes beyond SPECMAP by including processes in the tropics, including isolation forcing of monsoons, monsoon generation of a strong 23,000-year CH_4 signal, and the large 23,000-year tropical ocean SST response.

The first step in the analysis is to shift the phase of the SPECMAP $\delta^{18}O$ signal by 1500 years to incorporate the change in time scale noted earlier. This adjustment reduces the lags between insolation forcing and the SPECMAP $\delta^{18}O$ signals. All climatic proxies recorded in marine sediment cores and dated by reference to the marine $\delta^{18}O$ standard (SST, eolian fluxes, etc.) shift along with the $\delta^{18}O$ signal. The approach used here does not attempt a rigorous error analysis, but phase uncertainties of at least 1000 years are likely.

The next step is to assess possible offsets of the ice-volume signal from the SPECMAP $\delta^{18}O$ signal for each orbital period. The five cores used in the SPECMAP marine $\delta^{18}O$ stack come from the southern hemisphere and the tropics. If the SST trends in these cores have the same average phase as SPECMAP $\delta^{18}O$ for a given orbital period, the phase of the SPECMAP $\delta^{18}O$ signal can be considered a good indication of the phase of ice volume, regardless of the size of the SST overprint. In effect, an in-phase SST overprint cannot alter the phase of $\delta^{18}O$.

But if the average SST signal in the five cores leads SPECMAP $\delta^{18}O$ at a given period, it is likely that this "early" SST overprint has pulled the $\delta^{18}O$ signal toward an earlier phase, in which case the actual phase of ice volume must lag behind $\delta^{18}O$ to balance the SST lead. In such a case, the inference of a later ice-volume response can be independently confirmed if its phase matches that of ice-proximal responses such as North Atlantic SST. GCM experiments show that climate near and downstream from the northern ice sheets is strongly affected by their albedo and size and should closely follow the phase of the ice (Manabe and Broccoli, 1985; Rind et al., 1986).

With the phase of ice volume constrained in this way, and that of the insolation forcing well defined, the systems-analysis equation of Jenkins and Watts (1968) from Section 1 can be used to calculate a new time constant for the ice sheets. For internal consistency, the CLIMAP models required the same ice time constant for the ice responses to obliquity and precession forcing. This constraint is also required here.

Another major focus of the approach used here is the orbital-scale climatic roles of CO_2 and CH_4. The cyclic variations of these gases clearly reveal a link to external orbital changes (Petit et al., 1999), but until this point it has been unclear whether these gases act as forcing or feedback within the climate system. This analysis makes that distinction for each orbital period.

In some instances, a technique from trigonometry is used to infer how a signal at a given phase could result from the "influence" of two other signals with different phases. Most climatic signals examined here differ in phase by less than 90°. Adding together two component sine waves separated by 40° and having amplitudes of 3 and 1 produces a combined sine wave with a phase 3 times closer to the larger-amplitude wave than to the smaller one (Fig. 9). In effect, the larger amplitude of the first wave exerts a proportionally larger influence on the phase of the resulting wave, so that the relative phase offsets are the inverse of the relative amplitudes.

This approach can be inverted in a simple but useful way. If the phases of the three waves in Fig. 9 are known, but not their amplitudes, the relative amplitudes of the two component waves can be directly inferred

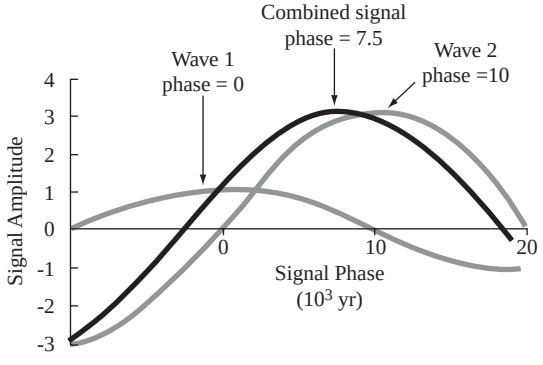

Fig. 9. If component sine waves with different amplitudes (wave 1 with amplitude 1 and wave 2 with amplitude 3) are added together to form a combined sine wave, the relative influence of the component waves can be ascertained from the phase of the combined wave, which lies 3 times closer to the larger-amplitude component wave than the smaller-amplitude one.

from the phasing of the combined wave relative to the component waves. This analysis will be used here in two contexts: (1) to infer separate influences on the phase of the SPECMAP $\delta^{18}O$ signal, and (2) as a rough index of the relative strength of multiple forcing sources within the climate system.

4.2. The paced signal: eccentricity

The approach used here returns to the CLIMAP view of the 100,000-year $\delta^{18}O$ signal as a response *paced* by eccentricity through its modulation of the precession signal. The SPECMAP search for a systematic pattern of forcing and response at this period (Imbrie et al., 1993) is abandoned, because the most important 100,000-year climatic signals (CO_2, SST and $\delta^{18}O$/ice-volume) all fall near the phase of eccentricity (Fig. 7). As noted earlier, this convergence of phases leaves too little time separation for forcing and response of ice sheets with long time constants. But pacing of these 100,000-year signals remains a plausible explanation.

The next three sections deal with climate changes at each of the orbital periods. As in the SPECMAP project, these signals are examined separately because the external forcing is different in space and time for obliquity and precession, and negligible for eccentricity. In addition, the climatic responses and interactions at each orbital period also differ in fundamental ways.

5. Hypothesis: forcing and climatic responses for obliquity

As noted in Section 1, obliquity is the easiest orbital period to analyze, because the forcing choice is limited to summer or winter insolation. The analysis here follows Milankovitch's choice of northern hemisphere summer forcing. Because of the 1500-year shift in the SPECMAP time scale, the marine $\delta^{18}O$ signal lags 6500 years behind summer insolation (Fig. 10). But is the 41,000-year $\delta^{18}O$ signal a valid measure of the timing of ice-volume changes?

Two arguments suggest that it is. First, the 41,000-year phase of the average SST signal in the cores from the SPECMAP $\delta^{18}O$ stack is close to that of $\delta^{18}O$ (Imbrie et al., 1989). The two cores from high southern latitudes have SST amplitudes averaging 1.2°C and phase leads versus $\delta^{18}O$ averaging 1500 years, but the tropical Atlantic core used in the stack and a Caribbean core near the one used in the stack have SST amplitudes averaging 0.35°C and phase lags versus $\delta^{18}O$ averaging 5700 years. The larger SST amplitudes in the southern cores are almost exactly canceled by the larger SST phase lags of the tropical cores, and the vector sum of the SST signals should have very nearly the same phase as the $\delta^{18}O$ signal. As a result, ice volume should lag

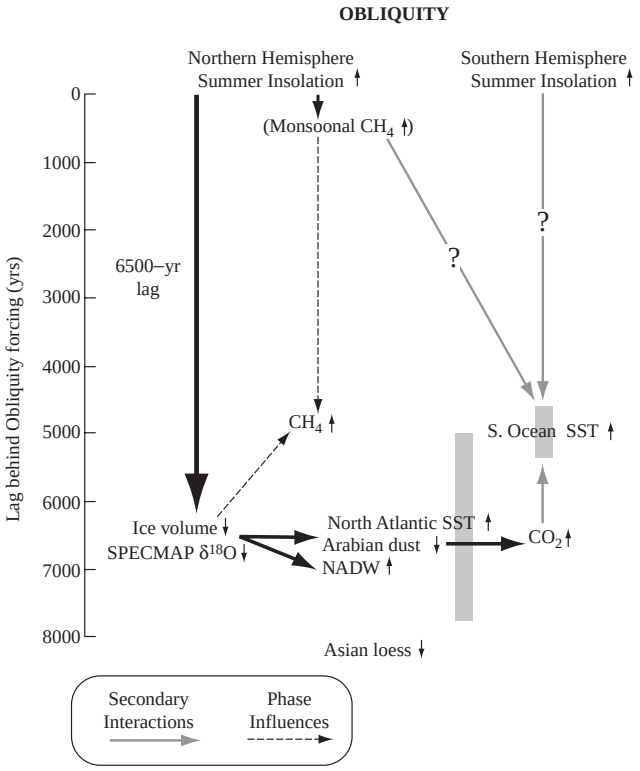

Fig. 10. Summer-insolation changes at the obliquity cycle force northern hemisphere ice volume with a lag of 6500 years. Ice-volume variations produce ice-proximal changes in SST, dust fluxes, and North Atlantic Deep Water flow, and some combination of these responses controls the 41,000-year atmospheric CO_2 signal. CO_2 provides a positive feedback that amplifies ice-volume changes. Small arrows indicate sense of response (increase or decrease) to increased summer insolation.

obliquity by roughly the same 6500 years as the $\delta^{18}O$ signal. Support for this argument comes from the phase of the 41,000-year CO_2, which is so close to that of the marine $\delta^{18}O$ signal at the obliquity period that it is unlikely to have shifted the $\delta^{18}O$ phase significantly.

Because ice volume is likely to have the same phase as the $\delta^{18}O$ signal, the equation from Jenkins and Watts (1968) can be used to calculate the ice time constant:

$$\phi = -\arctan 2\pi f T,$$

where ϕ is 57 (6500 years out of 41,000 years = 57° out of 360°) f is 1/41,000 years, and T is the time constant.

The ice-sheet time constant that satisfies this relationship is 10,000 years. In Section 6, this value will be tested in the context of changes in orbital precession.

Because the 41,000-year CO_2 signal is in phase with $\delta^{18}O$/ice volume (Fig. 10), it cannot be an independent source of forcing for the ice sheets. For this to be the case, the ice response would have to lag well behind the CO_2 forcing (in fact by 6500 years for a time constant of 10,000 years). Instead, the in-phase relationship observed suggests that the ice sheets control the CO_2 signal

with minimal or no lag and that CO_2 then acts as a positive feedback on the size of the ice sheets.

Several ice-driven responses in Fig. 10 have 41,000-year phases that make them plausible candidates for this ice-sheet control on atmospheric CO_2. Dust from the continents is thought to "fertilize" oceanic planktic algae that fix carbon and send it from surface waters to the deep ocean (Martin, 1990). Dust fluxes match prominent glacial isotopic stages (2, 4, 6) at the 41,000-year cycle in the North Pacific (Hovan et al., 1989), the northern Indian Ocean (Clemens and Prell, 1990), and in Vostok ice (Petit et al., 1999). These phase relationships suggest greater dust-driven carbon export to the deep sea (causing lower CO_2) during 41,000-year maxima in ice volume.

A second possible explanation is changes in Southern Ocean alkalinity caused by variable flow of North Atlantic Deep Water (Broecker and Peng, 1989). Because the transit time of NADW through the Atlantic is about 100 years (Broecker, 1979), changes in NADW formation are registered in the southern Ocean with little lag. When NADW flow slows or ceases, more $CaCO_3$ dissolution occurs on the Atlantic sea floor, more entrained CO_3^{-2} ions reach the Southern Ocean, and more surface-water CO_2 is neutralized. The decrease in surface-water CO_2 causes atmospheric CO_2 concentrations to drop. The % NADW signal in Fig. 10 (from Raymo et al., 1990) has the correct sense and phase to contribute to CO_2 variations at 41,000 years.

A third possible factor is the effect of SST cooling at high northern latitudes on CO_2 solubility. The observed cooling in the subpolar Atlantic ranges from 2°C to 4°C over roughly 5% of the world ocean surface. A global-mean surface-ocean cooling of 0.15°C (3°C × 0.05) would account for a CO_2 drop of 1–2 ppm, although simultaneous cooling of the North Pacific and of lower northern latitudes could increase this total.

Still another possibility is increased "pumping" of carbon from surface waters to the deep ocean in upwelling regions (Broecker, 1982; Sarnthein et al., 1988; Mix, 1989). The major upwelling regions in the northern hemisphere are near the California and Canaries Currents, although both are somewhat distant from the direct climatic impacts of the northern ice sheets.

In summary, the critical sequence of interactions at the obliquity cycle is ice-related. Northern hemisphere summer insolation forces a lagged ice-volume response, and northern hemisphere ice sheets control ice-proximal responses (North Atlantic SST, North Atlantic Deep Water formation, and dust fluxes) with little or no lag. Through these processes, ice sheets control changes in atmospheric CO_2 at the 41,000-year cycle. This direct control of CO_2 levels by ice sheets will re-emerge as a key part of the interpretation of the 100,000-year signal in Section 7.

Other climatic responses shown in Fig. 10 are probably not part of the central sequence of 41,000-year changes. For example, the Southern Ocean SST signal lags well behind insolation forcing but leads ice $\delta^{18}O$/ice volume by about 1500 years. As explained in Section 3, this SST lead is not regarded here as part of a critical train of responses (as it was by SPECMAP), both because it does not match the phase of the climatically important CO_2 signal, and because the SST lead relative to the phase of northern hemisphere ice is too small to permit significant forcing and response. The observed phase of southern-hemisphere SST at the obliquity period probably results from a dominant control by the late-phased CO_2 signal (and perhaps by NADW heat content as well), combined with a secondary control by "early phased" obliquity variations in the southern hemisphere (which have the same phase as those in the north).

The weak 41,000-year CH_4 signal is phased more than 1000 years ahead of global ice volume (Fig. 10). Like Southern-hemisphere SST, its phase may result from the influence of two different processes: (1) a small "early" CH_4 response to obliquity forcing at high northern latitudes; and (2) a larger contribution from late-phased ice-driven processes in the northern hemisphere that suppress CH_4 emissions when ice sheets are large.

Several Vostok ice-core signals that were found to have concentrations of power at the period of obliquity (Petit et al., 1999) are not discussed here. The reason for this omission is that the timing of these responses needs to be further explored, as suggested by the following example. The D/H ratio (δD), used as an index of air temperature over Antarctica, is recorded in the solid (ice) phase at Vostok. When the gas-phase CH_4 signal from Chappellaz et al. (1990) is plotted against the solid-phase δD signal from Jouzel et al. (1990) for the upper 160,000 years of Vostok ice, all major δD and CH_4 peaks match fairly closely (Fig. 11). Also shown at the top of Fig. 11 are the age shifts in the CH_4 signal used to align it with July 30°N insolation to create the CH_4 time scale of Ruddiman and Raymo (2003) shown in Fig. 4. These small shifts, all lying well within the stated dating uncertainties of ice-flow models, bring out far greater 23,000-year power in the CH_4 signal than in previous time scales, much of it at the expense of 41,000-year power.

If the CH_4 time scale is correct, and if the solid-phase δD signal shifts by amounts comparable to the CH_4 signal, the δD signal will gain more 23,000-year power than it had in earlier time scales, probably for the most part at the expense of 41,000-year power. If so, the phase of the remaining Vostok δD changes at the 41,000-year signal should be re-evaluated. As the next section shows, the most convincing leads of regional southern-hemisphere responses compared to ice volume occur at the 23,000-year precession signal. It is critical to

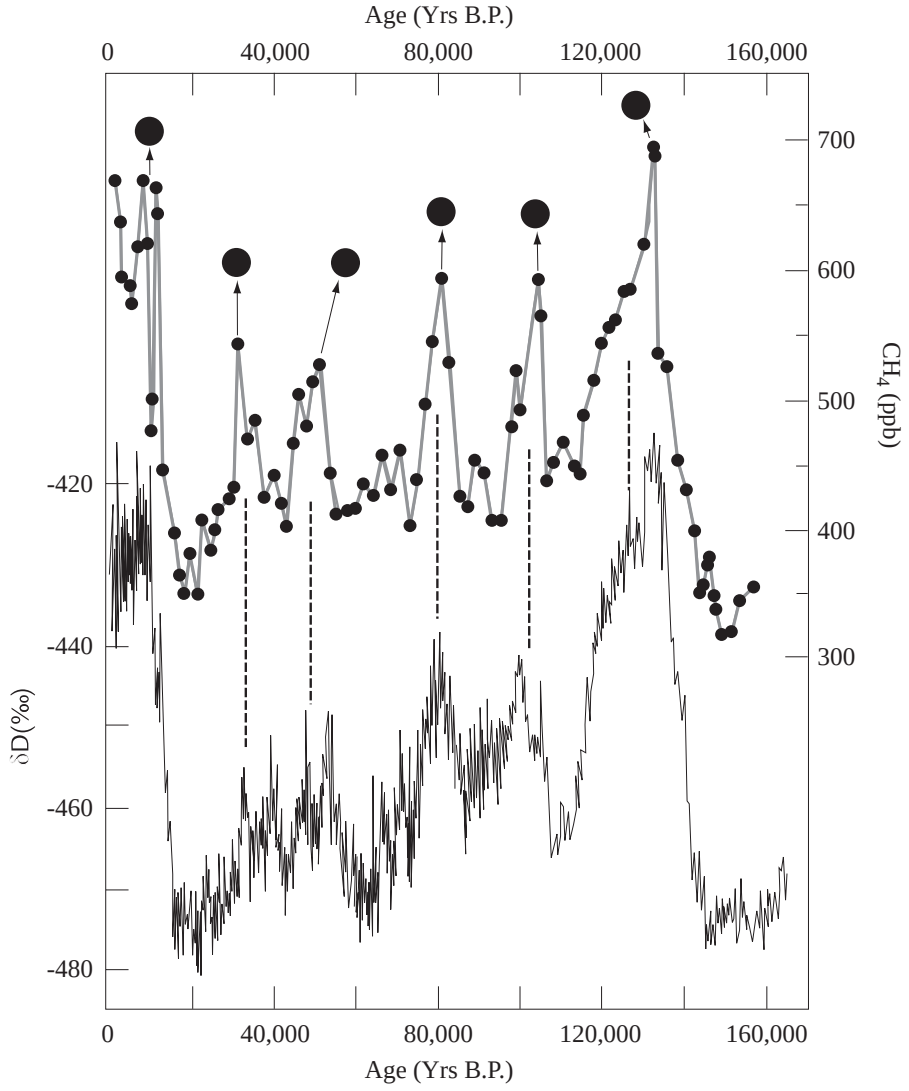

Fig. 11. Changes in CH_4 (Chappellaz et al., 1990) and δD in Vostok ice are plotted on the time scale of (Jouzel et al., 1990). The filled circles at the top show the changes in age of methane maxima required to create the Vostok CH_4 time scale of Ruddiman and Raymo (2003).

make sure that some of this 23,000-year lead has not appeared in previous 41,000-year signals as an artifact of small time-scale errors.

6. Hypothesis: precession forcing and climate responses

As noted earlier, orbital precession provides a range of incremental insolation "boosts" aligned to every season and month of the year. This synthesis accepts Milankovitch's choice of northern hemisphere summer as the critical forcing season but further specifies mid-July as the critical month. This choice makes physical sense because July is the time of greatest extent of snow-free land and these low-albedo land surfaces will most effectively absorb the extra increment of solar radiation provided by precession during July. Today, maximum heating of the continents occurs in July. This mid-summer heating also determines the phase of the Asian monsoon (Section 2).

With mid-July chosen as the key insolation season, the 10,000-year ice-sheet time constant calculated in Section 3 can be used to calculate a phase lag of ice volume of 4500 years behind this forcing for the period of precession. Independent confirmation of this choice comes from the fact that this lag positions the calculated ice-volume response at a phase lying in the middle of the wide range of North Atlantic SST (and NADW) responses (Fig. 12). Although these responses had lagged too far behind $\delta^{18}O$ (inferred ice volume) to agree with the SPECMAP model, they now have the same kind of in-phase relationship with ice volume as was the case for obliquity.

In solving one problem, however, at first it would appear this analysis has created another. Now the inferred ice-volume signal lags 2500 years behind that of

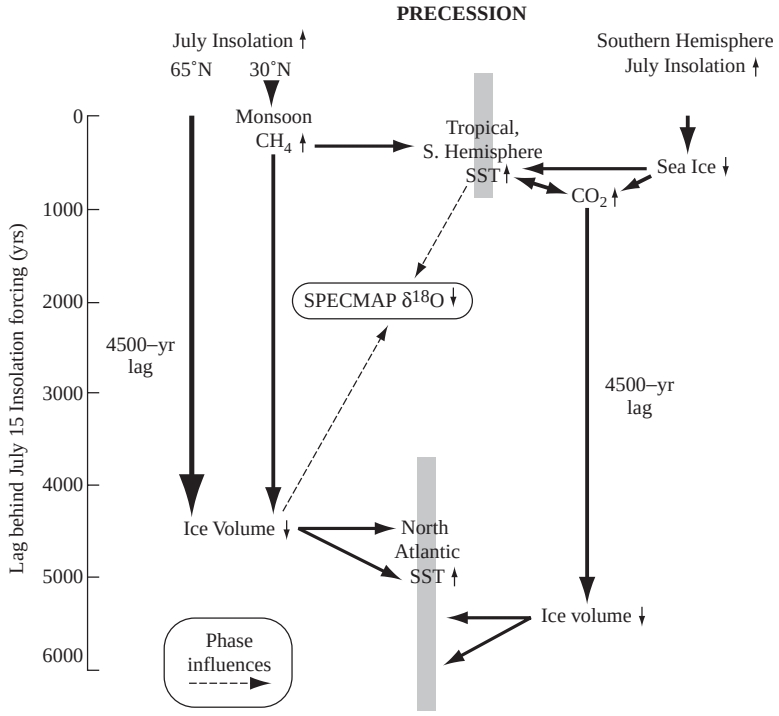

Fig. 12. July insolation forces northern hemisphere ice volume with a lag of 4500 years, and ice-volume changes control North Atlantic SST. July insolation also forces north-tropical monsoons and CH_4 changes with no lag, and it forces southern hemisphere sea ice, SST and CO_2 with a lag of up to 1000 years. Both CH_4 and CO_2 enhance the direct insolation forcing of ice volume. The phase of the SPECMAP $\delta^{18}O$ signal is a balance between an early SST signal and a late ice-volume signal. Small arrows indicate sense of response (increase or decrease) to increased summer insolation.

SPECMAP marine $\delta^{18}O$. The only way to explain this ice-volume lag versus $\delta^{18}O$ is by invoking a counterbalancing "early" influence that is also embedded in the $\delta^{18}O$ signal in such a way that the combined phases add up to that of $\delta^{18}O$. An obvious candidate for an "early" influence is the SST response in the tropical and Southern Hemisphere regions from which the cores in the SPECMAP $\delta^{18}O$ stack came.

Based on independent transfer-function estimates, 23,000-year SST signals in the Southern Ocean, tropical Atlantic, and Caribbean SPECMAP cores lead $\delta^{18}O$ by 1200–2900 years (Imbrie et al., 1989), with an average lead of 2100 years. Alkenone-based SST estimates from the South Atlantic confirm this phasing (Schneider et al., 1995). This lead should be large enough to offset the inferred 2500-year ice-volume lag behind $\delta^{18}O$ if SST has at least as much influence on the amplitude of the $\delta^{18}O$ signal as ice volume.

The 23,000-year $\delta^{18}O$ signal has an amplitude of 0.18‰, or a total amplitude range of 0.36‰. In order for half of this signal to be caused by changes in SST, the average range of the 23,000-year SST signal in the SPECMAP stack would have to be 0.8°C. The four cores used in the SPECMAP stack have 23,000-year SST signals that range from 0.24°C to 2.6°C and average 1.16°C, enough to account for more than half of the $\delta^{18}O$ signal. It is not possible to calculate the precise impact because of unknown salinity overprints and depth-stratified or seasonally fluctuating preferences of the planktic species. But the amplitudes of these early SST signals are clearly large enough to validate the assumption that they offset a late-phased ice-volume signal in the stacked SPECMAP $\delta^{18}O$ record (Fig. 12).

To this point, this analysis of causal links in the climate system at the period of precession has emphasized parallels with obliquity. In contrast to the obliquity cycle, however, the CO_2 and CH_4 responses signals are phased well ahead of ice volume, rather than in phase with it. This "early" phasing indicates that these greenhouse gases play an active forcing role at the period of precession, rather than the feedback role at the obliquity cycle.

At first, it might seem that insolation forcing would overwhelm the effects of the greenhouse gases. The 23,000-year insolation signal has a mean range of variation of 30 W/m^2 while the 23,000-year changes of CO_2 and CH_4 provide less than 1 W/m^2 of forcing. But this kind of comparison is invalid. Insolation reverses sign seasonally, so that summer increases are offset by winter decreases, and conversely. The oceans, which store large amounts of the heat used to melt ice sheets, integrate these opposing forcings into a much smaller annual residual sum. In contrast, greenhouse gases force the ocean year-round by the same amount and so they play a more important role in forcing ice sheets than indicated by the W/m^2 comparison.

Because the 23,000-year CH_4 signal is in phase with July insolation, it should enhance the effect of insolation forcing of ice sheets, and produce the same 4500-year lag in ice response (Fig. 12). The large 23,000-year CH_4 signal may also impact climatic responses in other regions. For example, CH_4 changes are likely to be part of the forcing of the δD (air temperature) response at Vostok (Fig. 11). Raynaud et al. (1992) estimated that the total glacial–interglacial temperature impact of CH_4 accounted for 20–25% of the combined effects from CO_2 and CH_4. Most of this glacial–interglacial CH_4 signal is at 23,000 years (Fig. 4).

The origin of the 23,000-year CO_2 signal is a more complex problem that will be addressed later in this section, but its role in the climate system is similar to that of CH_4. With the 23,000-year CO_2 signal phased slightly behind July insolation and CH_4, the ice response to CO_2 forcing should also occur about 1000 years later, but still nearly in phase with insolation and CH_4.

The revised interpretation of 23,000-year ice-volume phasing in Fig. 12 requires an updated re-assessment of this part of the SPECMAP model. Now, the phase delay between CO_2 and the main ice-volume response is 3500 years, which is the same as SPECMAP predicted, rather than too close to the ice-volume response based on equating the ice phasing with $\delta^{18}O$, as in Section 3.

Still, serious flaws remain for the SPECMAP model at the precession cycle. The very first SPECMAP requirement is a 23,000-year response in the Nordic Sea region with an early phase, yet no long-term signal has ever been identified. Instead, every 23,000-year climatic response found in this region has the late phase of the ice sheets lying west and east of the Nordic Seas, or the even more delayed phase typical of ice-proximal responses in the North Atlantic and in North America and Europe south of the ice sheets.

The second problem with the SPECMAP model is the paucity of evidence from proxy measurements of strong 23,000-year variations in deep-water flow through the Atlantic Ocean pathway. Proxies of the percentage of northern-source (NADW) water in the deep flow based on $\delta^{13}C$ show large concentrations of 100,000-year and 41,000-year power with the late phase of the $\delta^{18}O$ signals, but little if any 23,000-year response (Raymo et al., 1990, 1997). One Cd/Ca record from 31°S show a small early phased 23,000-year signal, but another at 42°N has much stronger 41,000-year power, and "late" phases close to that of marine $\delta^{18}O$ for both obliquity and precession (Boyle, 1984). Other Cd/Ca records from southern hemisphere cores show relatively weak 23,000-year signals with differing phases that fall well before or well after the timing required by the SPECMAP model (Oppo and Rosenthal, 1994). In summary, no Atlantic deep-water proxy published to date has both a strong 23,000-year signal and an early phase.

6.1. Origin of "early" 23,000-year SST signals in the southern hemisphere

In marked contrast to the Arctic, strong 23,000-year signals with an "early" phase are pervasive in SST responses across the southern hemisphere and the tropics. A summary of SST responses by Imbrie et al. (1989) based on faunal transfer-function estimates showed a remarkably coherent pattern of early phased SST responses in every core from the southern hemisphere (mostly the Atlantic). Subsequently, SST estimates based on different methods (alkenone and Mg/Ca ratios) have confirmed the existence of this early 23,000-year response in the eastern South Atlantic boundary current (Schneider et al., 1995), the eastern tropical Pacific (Lea et al., 2000), and the western tropical Indian Ocean (Bard et al., 1997).

The observed lead of this SST signal with respect to marine $\delta^{18}O$ varies from 1200 to 2700 years, equivalent to a lead of 3700 to 5200 years relative to the newly inferred phase of ice volume shown in Fig. 12. This phasing is aligned with precessional insolation forcing in middle July to early middle August (northern hemisphere summer and southern hemisphere winter).

Forcing of this signal from high northern latitudes can be ruled out, because no evidence exists for an early phased signal in the north. Forcing by the Antarctic ice sheet is also implausible, because temperatures are too frigid over this ice sheet even in summer for it to be vulnerable to ablation caused by insolation. By process of elimination, the southern SST signal appears to be a "fast" response of some kind to insolation forcing in mid-July to mid-August.

The problem with invoking this explanation for the ocean-dominated southern hemisphere is that the slow precession of seasons around Earth's orbit offers a full array of insolation "boosts" for each season, with insolation maxima in one season balanced by opposing minima in the opposite season. It is thus necessary to explain why the ocean would single out and preferentially respond to forcing only in July–August. Three such processes are discussed below, all of which are consistent with the presence of this early phased 23,000-year SST signal at latitudes south of 10°N: (1) north-tropical monsoons; (2) forced alternation of tropical Pacific circulation between the El Nino and La Nina modes; and (3) sea-ice changes at high southern latitudes.

6.1.1. North-tropical monsoons

Building on the earlier CLIMAP work of Gardner and Hays (1976), McIntyre et al. (1989) identified a strong 23,000-year SST signal with an early July–August phase in the south-tropical Atlantic. One of two possible origins they cited was the effect of the North African monsoon in overriding the typical zonal flow of

southern winter trade winds in the Atlantic. In the proposed sequence, extra insolation heating of North Africa in northern hemisphere summer (July–August) at the precession cycle creates strong monsoons, diverts trade-wind flow into North Africa, suppresses the south-tropical divergence normally produced by zonal winds, and causes warmer SST along and south of the equator. The converse pattern (strong zonal trade-wind flow, strong divergence, and cold SST) occurs when precessional insolation minima occur in July–August. Because the North African monsoon has the same 23,000-year phasing as the Atlantic SST signal, it offers a way to make the southern trade winds in the tropical Atlantic sensitive to precessional insolation "boosts" aligned with that season. The major limitation of this concept is that monsoon forcing seems unlikely to affect the entire southern hemisphere.

6.1.2. *El Nino and La Nina*

Changes in the relative frequency of the El Nino and La Nina circulation modes in the tropical Pacific could also contribute to the early 23,000-year SST response. The La Nina state resembles the cold extreme of the 23,000-year response, with a strong subtropical high in the south Pacific, a vigorous Peru Current, and a strong equatorial divergence. These phenomena are most strongly manifested today at the end of southern hemisphere winter (in August) as an amplification of the typical seasonal pattern. The El Nino state resembles the warm extreme of the 23,000-year SST response, with opposite trends in all the above indices. In principle, these two patterns might be favored as more permanent modes of tropical Pacific circulation if aligned with precessional insolation in a sensitive season.

Clement et al. (2001) tested an El Nino model forced by changes in precessional insolation forcing and found little systematic response. If anything, their model showed a tendency for enhanced July–August insolation at the precession period to suppress the El Nino pattern, and this sense of change is opposite to 23,000-year SST changes in an eastern tropical Pacific core, which shows warmest SST values during precession insolation maxima (Lea et al., 2000). It is also unclear that an El Nino explanation can account for the strong 23,000-year SST signals in areas of the Atlantic and Indian Oceans and high southern latitudes far from ENSO changes.

6.1.3. *Southern sea ice*

The major shortcoming of the first two explanations is that they fail to explain the pervasiveness of the early 23,000-year SST signal across the entire southern hemisphere. Most of the strongest SST responses occur in regions directly affected today by wind-driven flow around winter subtropical high-pressure systems: the middle latitudes of the Southern Ocean, eastern boundary currents, and eastern divergences. This pattern suggests that the origin of the southern SST signal lies in a process capable of spinning up all of these high-pressure cells. Support for this inference comes from faunal SST estimates in the eastern tropical Atlantic showing that the largest SST changes occur in southern winter (Mix et al., 1986; McIntyre et al., 1989), the time of maximum strength of the southern subtropical highs.

Hays et al. (1976a, b) and Gardner and Hays (1976) first invoked a large-scale wind-driven response from the southern hemisphere to explain SST changes in the tropical Atlantic. Others have subsequently concurred (McIntyre et al., 1989; Labeyrie et al., 1996; Mix, 1996; Brathauer and Abelmann, 1999). Hays et al. (1976a, b) and Gardner and Hays (1976) further proposed that southern hemisphere wind strength might be tied to changes in the extent of Antarctic sea ice.

The change in state from seawater to sea ice is the kind of climatic discontinuity that might produce a preferred seasonal response. An ice-covered ocean absorbs little solar radiation, but it can absorb large amounts if ice-free. Sea ice also has a large potential to amplify climate change. Seawater at the freezing point releases enough heat to keep surface air temperatures near 0°C, but an ocean entirely covered with ice allows air temperatures to fall to −20°C or below. Covering the ocean with ice makes it function much like land in a thermal sense.

Nicholson and Flohn (1981) noted that Antarctic sea ice is a major factor in the strong seasonal changes of the modern southern hemisphere. Because of seasonal changes in radiation, sea-ice cover varies from 20 million km^2 in winter to 3 million km^2 in summer, with most of the summer cover sustained by cold winds draining off the Antarctic ice sheet (Zwally et al., 1983). They also pointed out that the seasonal increase in the extent of sea ice compresses the zonal thermal gradient. The resulting northward shift of the westerlies spins up flow in the subtropical high-pressure cells and thereby intensifies atmospheric winds at middle and even lower latitudes. These responses are ultimately caused by seasonal decreases in insolation, but they are significantly amplified by sea ice. The relaxation of the high-pressure systems in summer is ultimately due to higher insolation, but aided by the large poleward retreat of sea ice.

By analogy, orbital-scale variations in the northern winter limit of sea ice driven by precessional insolation forcing should be felt across the entire southern hemisphere. The fact that the largest observed SST changes at the 23,000-year cycle lie in regions of wind-driven divergence fits this explanation. But this proposed mechanism raises three questions.

First, why would winter sea ice respond mainly to variations in precessional insolation, when obliquity changes are important at high latitudes? The answer

may be the darkness of the winter polar nights (Fig. 13). The latitudes where obliquity is important in the summer season (poleward of 66.5°S) lie in darkness during winter, and the weak obliquity forcing just equatorward of the Antarctic Circle arrives at very low sun angles. In contrast, stronger precessional insolation changes occur near the modern limit of winter sea ice and above the ice-free waters just to the north.

Second, why would the sea-ice limit be controlled by winter insolation? Should not the greater absorption of summer insolation by an ice-free ocean control the orbital timing of sea-ice changes? A plausible answer to this question comes from considering the situation today: the Antarctic ice sheet sets the "thermostat" of the southern hemisphere at so cold a level that sea ice forms each winter no matter how much or how little radiation was absorbed by the ocean the previous summer. If extensive winter sea ice is destined to form under "normal" conditions, it follows that the northern limits to which sea ice will reach in a given winter should be sensitive to the amount of radiation received by the ocean near and north of the sea-ice limits during that season (July–August).

It is not possible to estimate the impact of winter insolation changes on orbital-scale variations in winter sea-ice limits because of the very complex dynamics of Southern Ocean circulation, but a comparison to seasonal changes is instructive. Today, seasonal insolation changes of $135 \pm 15\,W/m^2$ force the seasonal sea-ice limits back and forth between about 57° and 70°S (an area of 17 million km^2). At orbital time scales, changes in precessional insolation during winter vary over a range of 15–30 W/m^2 in the same regions. This comparison suggests that the response of the winter sea-ice limit to precession-driven changes in insolation could be substantial.

Third, and finally, if winter sea-ice extent is the mechanism that projects changes in wind strength and SST across the southern hemisphere, why are the SST changes in phase with insolation changes between July 15 and August 15, rather than with the modern September sea-ice maximum (Zwally et al., 1983)? The answer to this question is unknown. Perhaps the July–August phase is influenced by a combination of all three processes: the monsoon maximum reached in mid-July, the sea-ice maximum reached in September, and the ENSO circulation extreme in August.

In summary, a strong and early 23,000-year SST response exists throughout the southern hemisphere, whatever the exact combination of factors that accounts for its origin. In contrast to the absence of any such a signal in the northern hemisphere, the prevalence of this early 23,000-year signal in the south suggests that any early 23,000-year response detected in deep-water flow through the Atlantic Ocean probably records changes in flow that originate in the south, rather than in the north (Imbrie et al., 1992).

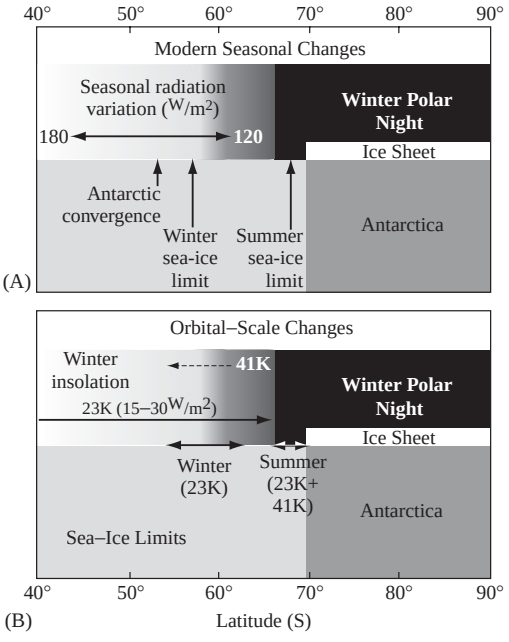

Fig. 13. (a) Southern hemisphere sea ice varies seasonally across an area of 17 million km^2 because of seasonal changes in solar radiation. (b) Orbital-scale changes in insolation of 15–30 W/m^2 near the winter sea-ice limit occur primarily at the 23,000-year period of precession. In winter, the high latitudes where obliquity normally is strongest are in the darkness of polar night.

6.2. *Southern hemisphere origin of the 23,000-year CO_2 signal*

An obvious starting point for explaining the early CO_2 response at the 23,000-year cycle is the similarly phased changes in southern-hemisphere SST. Because the solubility of CO_2 in seawater is greater at lower temperatures, an early SST cooling will reduce atmospheric CO_2. In addition, the opposing effect of ocean salinity on CO_2 tied to freshwater storage in ice sheets will be delayed thousands of years behind the SST-induced changes (Fig. 12).

Changes in CO_2 at the 23,000-year cycle have an average range of about 15 ppm (Fig. 5), and a 15-ppm CO_2 change would cause a global-mean SST change of 1.2°C (for a $2\times$ CO_2 equilibrium sensitivity of 2.5°C). The observed 23,000-year SST cooling in thermally reactive regions of the southern hemisphere ranges from 1°C to 4°C and averages 2.5°C (Hays et al., 1976a; McIntyre et al., 1989; Schneider et al., 1995; Lea et al., 2000). Transfer-function estimates of SST changes in regions remote from ocean divergences indicate SST changes of less than 1°C (Imbrie et al., 1989), but estimates from the alkenone and Mg/Ca methods indicate changes of 1–2°C (Bard et al., 1997; Lea et al., 2000).

It is impossible to estimate accurately the mean southern-hemisphere SST response from this core coverage, but the available data indicate it exceeds 1°C and might well be as large as 1.5°C. The southern hemisphere ocean (and tropics north to 10°N) accounts for more than 70% of the area of the global ocean. The global-mean amplitude of this "early" SST signal is thus likely to be at least 0.7°C (1°C × 0.7), and possibly larger. If so, the observed early phased southern-hemisphere SST cooling at the 23,000-year period accounts for a large part of the observed CO_2 signal.

The rest of the 23,000-year CO_2 response could result from direct sea-ice control of CO_2 ventilation (Stephens and Keeling, 2000) and from carbon pumping in wind-driven divergences in eastern boundary currents and along the equator (Broecker, 1982; Sarnthein et al., 1988; Mix, 1989). In contrast to the obliquity cycle, dust-flux fertilization of the ocean is not a promising explanation of these CO_2 changes. The Arabian dust fluxes, Asian loess records, and Vostok dust record all have weak 23,000-year signals.

In summary, ice-volume changes at 23,000 years result from combined forcing by northern hemisphere summer insolation and greenhouse gases. The CH_4 changes originate from northern summer forcing of tropical monsoons, while the CO_2 changes result from winter insolation forcing of southern hemisphere climate through several possible mechanisms.

The timing of these 23,000-year greenhouse-gas signals complicates interpretations of changes in southern hemisphere climate based on pollen (vegetation) and on fluctuations of mountain glaciers. At the precession period, these indicators respond to summer insolation forcing with a December/February phase, but to greenhouse-gas forcing with an opposing July–August phase.

7. Hypothesis: eccentricity pacing of 100,000-year climatic responses

The strong 100,000-year climatic cycles of the last 0.9 Myr pose a different problem from those at the periods of obliquity and precession. Direct insolation changes at the period of orbital eccentricity are minimal, less than 0.15% of the amplitude of those at precession. The SPECMAP model (Imbrie et al., 1993) attempted to overcome this shortfall in external forcing by invoking an undefined source of internal thermal forcing (Section 1, Fig. 3). The SPECMAP interpretation rested largely on the observation that large 100,000-year phase offsets existed among different responses in the climate system, but the evaluation of the effect of rectification on phase in Section 3 shows that most of these responses actually lie very close to the phase of eccentricity.

With the very early 100,000-year phase for the Southern Ocean SST signal rejected as an artifact of rectification, and with less than 5000 years between the phase of CO_2 and that of marine $\delta^{18}O$ (Fig. 7), too little phase separation remains to accommodate the long train of forcing and response required by the SPECMAP model based on a 15,000-year ice time constant (Fig. 3). In the hypothesis developed below, eccentricity modulation of precession is assumed to pace the phase of all responses in the climate system. Forcing and response do exist in this hypothesis, but do not occur at a cycle of 100,000 years.

7.1. The origin of 100,000-year climatic cycles

The hypothesis presented here is that the 100,000-year cycle results from external orbital pacing of climate-system interactions initiated by orbital forcing at the periods of obliquity and precession (Figs. 10 and 12). Greenhouse gases play key roles in creating the 100,000-year cycle by enhancing insolation forcing at the period of precession and by amplifying ice-sheet responses at the period of obliquity. Eccentricity modulation paces the 100,000-year climate system by determining times when internal enhancement of the precession cycle drives the climate system toward an interglacial state, and times when internal amplification of the obliquity cycle drives it toward a glacial state.

The strong 100,000-year power observed in global climatic responses such as marine $\delta^{18}O$ is created from the four signals shown in Fig. 14. Two of these signals are the linear ice-volume responses to insolation forcing at obliquity and precession (with lags of 6500 and 4500 years, respectively). The third signal is the positive feedback of CO_2 to ice volume at the 41,000-year obliquity rhythm (the example shown is based on Arabian Sea dust fluxes from Clemens and Prell, 1990). The fourth signal is the forcing of ice volume caused by the combined effects of CO_2 and CH_4 at the 23,000-year precession cycle (Fig. 12).

The 100,000-year cycle can be explained by four processes summarized in Figs. 15 and 16:

(1) *Alignment of insolation forcing at the 23,000-year and 41,000-year cycles causes major transitions in the mean climatic state*. This concept has been implicit in orbital theory since Milankovitch (1941). As shown in Fig. 15 (left), the last two terminations occur near 11,000 and 128,000 years ago, times of close alignment of obliquity and precession insolation maxima. Imbrie et al. (1993) further noted that interglacial-to-glacial transitions occur as linear responses to close alignment of obliquity and precession insolation minima. The most recent such alignments, at 75,000 and 190,000 years ago, account for the timing of the Isotopic Stage 7/6 and 5/4 boundaries. [Note—use of the term "state" in this discussion is not meant to imply the existence of distinct climatic "modes" in a bistable system, but simply the

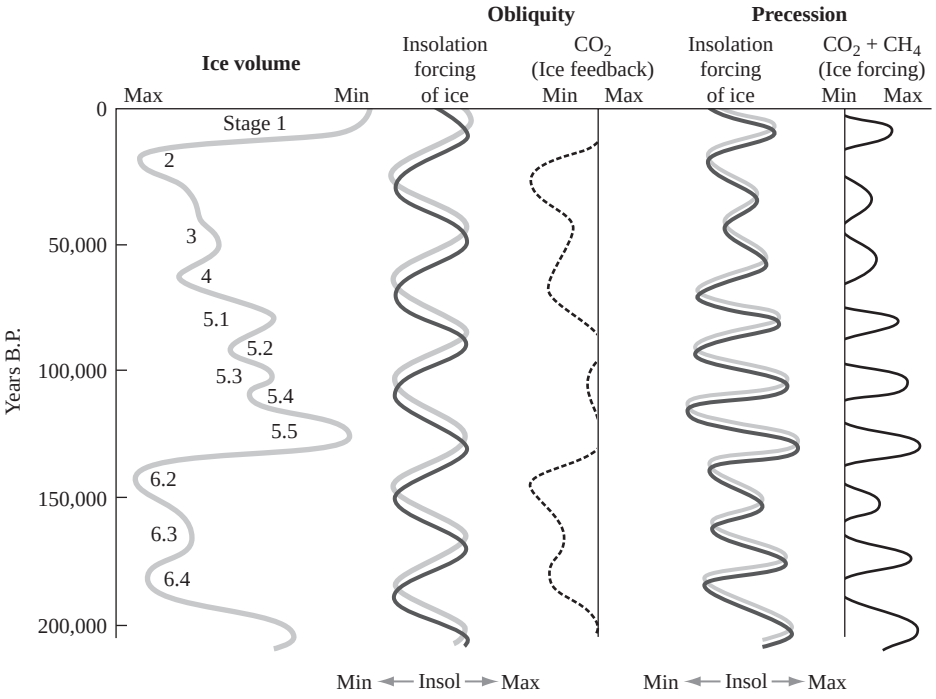

Fig. 14. (Left to right) The 100,000-year signal of $\delta^{18}O$ (~ice volume) can be evaluated as a combination of: the linear response of ice volume to obliquity forcing; CO_2 amplification of the 41,000-year ice-volume response by ice-driven processes (represented here by dust fluxes to the Arabian sea); the linear response of ice volume to precession forcing; and enhanced forcing of ice volume by 23,000-year changes in CO_2 and CH_4.

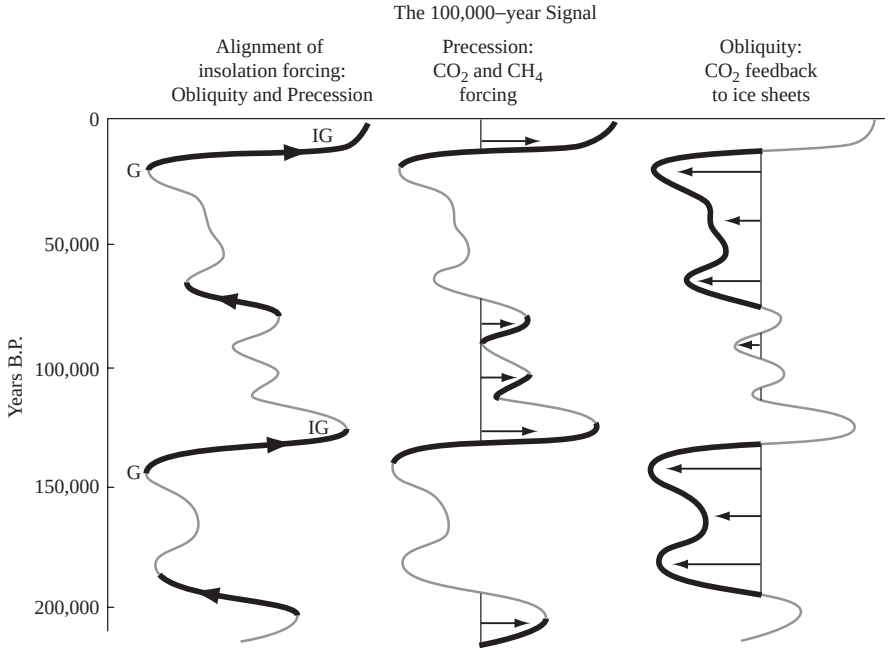

Fig. 15. Factors contributing to the form of the 100,000-year climate signal: (left) alignment of forcing by obliquity and precession; (center) enhanced precession forcing toward an interglacial climatic state by CO_2 and CH_4; and (right) CO_2 feedback that amplifies ice-volume maxima at the obliquity cycle and disappears early on terminations.

general tendency of the system toward a glacial or an interglacial climate.]

For a transition of climatic state to occur, extremes of obliquity must be aligned with precession extremes of sufficient size such that the combined insolation forcing is large. The obliquity signal approximates the shape of a sine wave, so that no individual cycle is highly favored over another, but eccentricity modulation produces

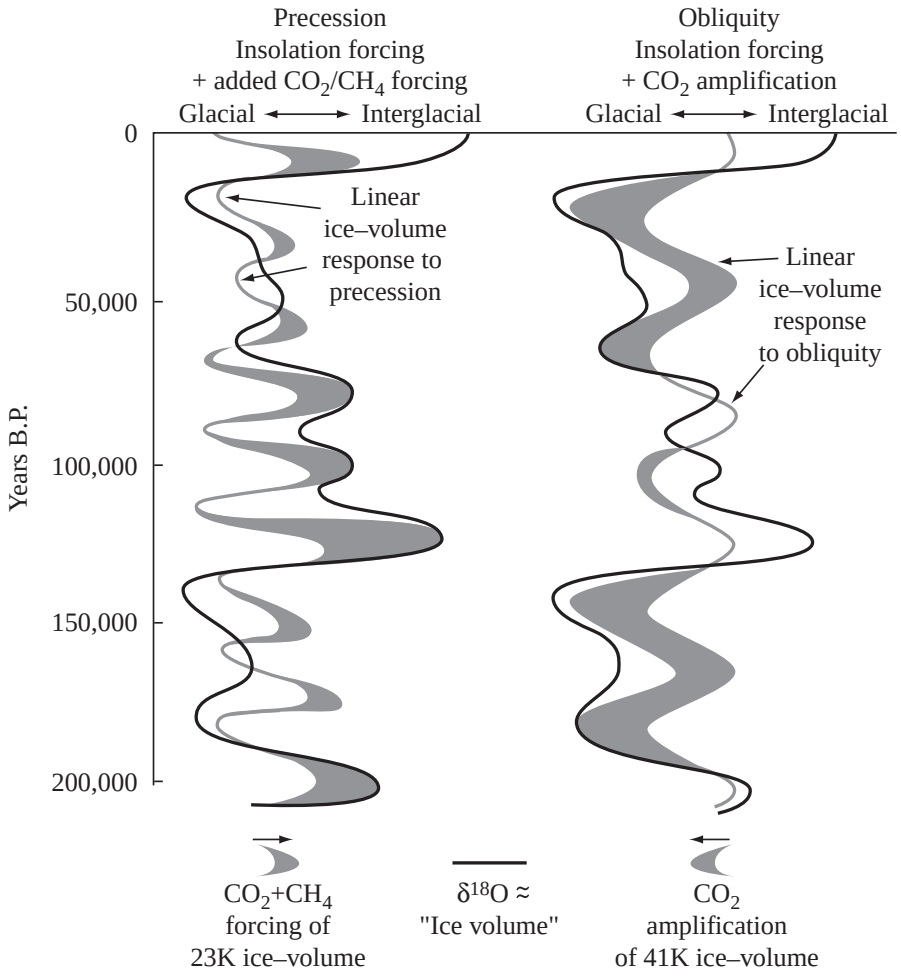

Fig. 16. (Left) At the precession cycle, CO_2 and CH_4 maxima enhance linear insolation forcing of ice volume and drives climate toward an interglacial climatic state. (Right) At the obliquity cycle, CO_2 feedback amplifies 41,000-year ice-volume maxima created as a linear response to insolation minima and drive climate toward a glacial state.

widely varying amplitudes in precession maxima and minima in clusters separated by 100,000 years. As a result, alignment of obliquity extremes with high-amplitude precession extremes occurs at average intervals of 100,000 years. For reasons discussed later and recognized by Broecker (1984) and Raymo (1997), major transitions from the glacial to the interglacial state only occur after an interval of several low-amplitude precession maxima. In addition, transitions from the interglacial to the glacial climate state occur near the end of clusters of large precession maxima. In this way, eccentricity paces major transitions in climate state.

Alignment of obliquity and precession can cause climatic transitions, but it cannot keep climate in the new configuration. Because insolation at both of these periods varies around a mean, the system will come back to that mean unless additional processes work to maintain the new state.

(2) *Greenhouse gases, by enhancing insolation forcing from precession, help to hold the climate system close to an interglacial state*. Large insolation maxima that occur at the precession cycle in clusters spaced at 100,000 years can melt large volumes of ice, because ablation rates at warm temperatures are higher than accumulation rates at cold temperatures (Oerlemans, 1991). Because CH_4 and CO_2 maxima are nearly coincident with insolation maxima (Fig. 12), greenhouse-gas changes enhance this insolation forcing and push climate farther into an interglacial state (Fig. 15, center; Fig. 16, left). The persistence of an interglacial state is favored through several precession cycles by poor alignment of insolation minima at precession and obliquity. But once precessional insolation maxima grow smaller and ablation is reduced, the system can no longer be held in an interglacial state. It then becomes vulnerable to the next close alignment of obliquity and precession minima, which will shift the system toward or into a glacial state.

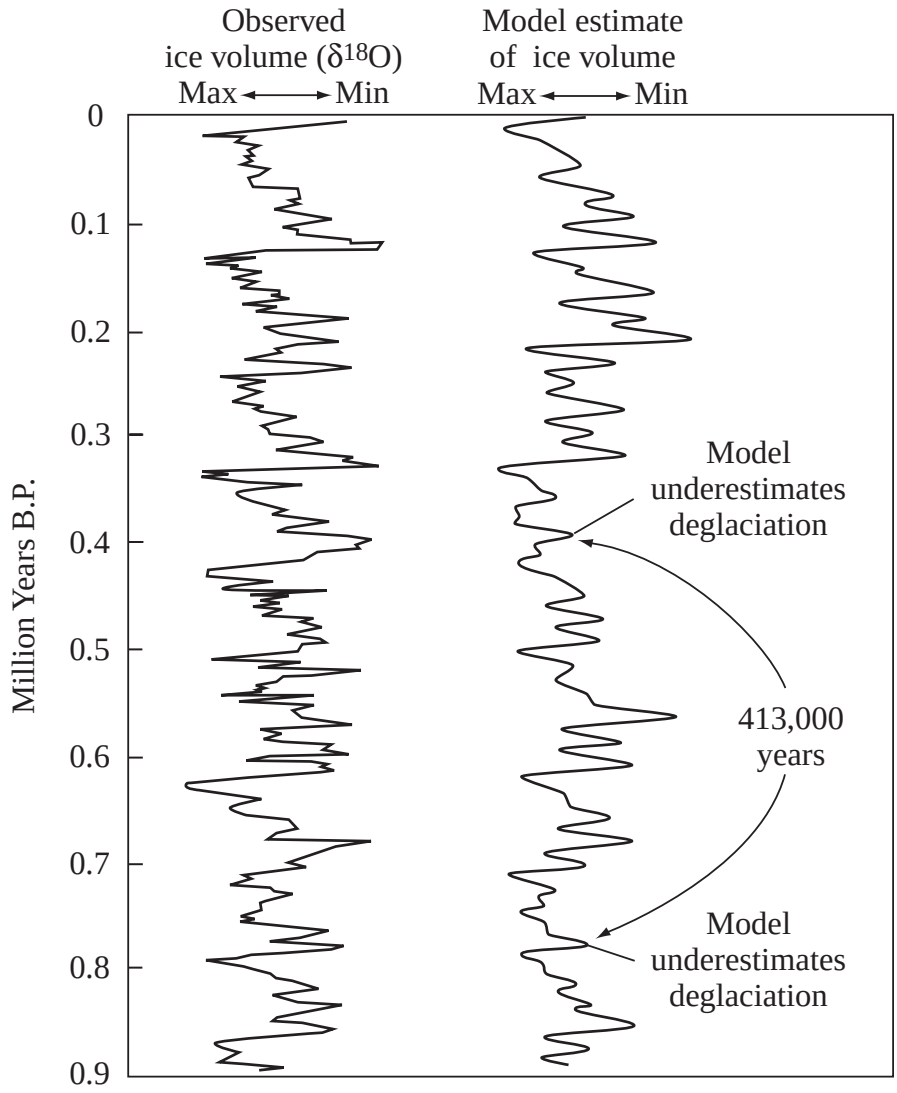

Fig. 17. The numerical model of Imbrie and Imbrie (1980) produces a 100,000-year saw-toothed ice-volume signal (example from Bassinot et al., 1994). The model is based on the assumption that ice sheets melt four times faster than they grow in response to orbital insolation forcing.

A similar process was implicit in the numerical model of Imbrie and Imbrie (1980), which used summer insolation forcing at 65°N as the input function and generated a 100,000-year signal with a good resemblance to the target $\delta^{18}O$ (ice-volume) signal. A more recent application of this model is shown in Fig. 17. In effect, this modeling exercise demonstrated that a 100,000-year signal can arise from eccentricity pacing of forcing responses at the periods of obliquity and precession, without any requirement for a distinct 100,000-year framework of forcing and response.

The key parameterization in this model—constraining the ice sheets to melt four times as fast during deglaciation as they accumulate during ice growth—was an over-simplification. Actual ice sheets at subpolar latitudes have large zones of slow accumulation balanced by smaller zones of rapid ablation, and shifts in this balance allow net melting or accumulation of ice. Even during the intervals when summer insolation begins to increase toward the next precession maximum, the ice sheets tend to keep the local climate cold and close to a glacial state by their own effects on climate. This effect, especially the great height of glacial-maximum ice, makes the model parameterization unrealistic: how can the same ice melt four times faster during the still-cold climatic state just after a glacial maximum than it accumulates in the similarly cold state just before the maximum?

The 23,000-year phase of the greenhouse gases (Fig. 14) adds an in-phase forcing toward warmer conditions that should mimic the over-simplified model parameterization but in a realistic way. Both CH_4 and CO_2 are generated in regions far from the retarding effects of the ice sheets. Because they are atmospheric

gases, their warming effects are projected into the ice-sheet regions and can enhance the impact of insolation forcing.

In summary, supplemental 23,000-year forcing from greenhouse gases helps precessional insolation forcing keep the climate system in an interglacial state. In addition, the extra forcing provided by CH_4 is rectified such that methane maxima fully track the amplitude of insolation maxima, but the minima only partly track the size of insolation minima. This helps keep the climate system in an interglacial state when eccentricity is high.

(3) *CO_2 feedback at the obliquity cycle drives the climate system deeper into a glacial state.* CO_2 feedback to ice sheets produces an added boost toward the glacial climatic state when eccentricity modulation of precession is weak (Figs. 15 and 16, right). Ice sheets never reach sufficient size during interglaciations to generate large CO_2 feedback, but they become capable of doing so when eccentricity decreases and precessional melting events weaken. Once the close alignment of obliquity and precession minima permits a switch to a glacial state, ice sheets become large enough to generate their own CO_2 feedback and keep the climate system in a glacial state. Again, eccentricity modulation of precession provides the pacing for this response.

CO_2 feedback at the obliquity cycle apparently arises from processes such as dust fertilization of ocean algae, NADW suppression, and SST cooling (Fig. 10). Both the dust-flux and NADW signals are rectified, with large responses during glacial climates, but little variation during interglacial climates (Fig. 14). The shape of these signals suggests that ice sheets may generate maximum CO_2 feedback only when they exceed a certain size. Consistent with this idea, the clearest indicators of an obliquity signal in the last two 100,000-year $\delta^{18}O$ cycles are glacial Isotopic Stages 2, 4, 6.2, and 6.4, all of which are expressions of the 41,000-year signal (Fig. 14).

The absence of large precession insolation maxima and the poor alignment of obliquity and precession also help to maintain the glacial state. Obliquity insolation maxima that occur during the glacial climatic state (such as in Isotopic Stage 3) tend to push the climate system toward the mean climatic state, but millennial-scale fluctuations like those in Isotopic Stage 3 hold the climate system closer to the glacial state. Dust-flux fluctuations evident in high-resolution ice cores (Dansgaard et al., 1984), episodic suppression of NADW flow (Keigwin and Boyle, 1999), and surface-ocean temperature oscillations (Bond et al., 1993) may briefly provide levels of CO_2 feedback typical of full-glacial conditions even during obliquity insolation maxima.

(4) *Terminations occur when all major forcings act on large masses of ice.* The three above factors appear to account for the basic "square-wave" shape of many 100,000-year climatic cycles (the existence of interglacial Stages 5, 7 and 9 versus glacial Stages 2–4, 6, and 8). In addition, they explain part (and potentially all) of the large volume of ice melted on terminations, the central feature of sawtooth-shaped 100,000-year cycles. As noted above, several forcing signals come together at, and only at, those times: coincident maxima in insolation at the periods of obliquity and precession, as well as maxima in the 23,000-year CO_2 and CH_4 signals.

In addition, additional forcing appears to be available from the removal of the 41,000-year CO_2 "ice-feedback" signal early on terminations. Removal of this positive feedback favoring glaciation is equivalent to an extra impetus toward deglaciation. On average, the CO_2 feedback at the 41,000-year cycle has the same phase as ice volume (Fig. 10), but this relationship apparently breaks down on terminations. Two of the ice-proximal responses with the correct phases to account for the 41,000-year CO_2 feedback—dust fluxes and NADW suppression—did not slowly diminish in strength during Termination I, as would be expected for a 41,000-year sine wave lagged 6500 years behind insolation forcing. Instead, dust fluxes in high-resolution Greenland ice cores abruptly decreased to near zero at 14,600 years ago (Mayewski et al., 1996), and production of North Atlantic Deep Water increased abruptly just after 14,500 years ago (Keigwin and Lehman, 1994).

These abrupt shifts imply that the 41,000-year CO_2 signal shifted into the interglacial state early on the last termination and remained there throughout, except for a brief reversion during the Younger Dryas event. As a result, all five major insolation and greenhouse-gas forcings toward the interglacial state achieved maximum expression very near the time of alignment of the insolation maxima. Numerical modeling will ultimately be required to determine whether this focusing of multiple forcings during terminations is sufficient to account for the amount of ice melting that actually occurred, or whether internal amplifications by processes such as the vulnerability of marine ice sheets to sea-level rise or delayed bedrock rebound are also required.

These observations also provide a new perspective on an old problem: the synchronous responses of the northern and southern hemispheres at terminations (Broecker and Denton, 1989). Four of the five factors just discussed have the same phasing in both hemispheres—CO_2 at 41,000 and 23,000 years, CH_4 at 23,000 years, and summer insolation at 41,000 years. Only precessional insolation is out of phase between the hemispheres, and the relationships discussed in Section 5 indicate that July is the critical season of insolation forcing for both hemispheres, even though July is mid-summer in the north and mid-winter in the south. If July is critical in both hemispheres, precessional insolation joins the other four factors in predicting in-phase climatic changes in the two hemispheres, as observed. The synchronous response of the two hemispheres makes sense.

To this point, the hypothesis presented here has focused on the origin of the 100,000-year signal in northern ice sheets, but not on the greenhouse gases. Ice sheets can project their 100,000-year responses into ice-proximal regions of the northern hemisphere, but not into more distant regions. To explain the presence (and often dominance) of 100,000-year signals in other regions presumably requires forcing from greenhouse-gas changes at this period.

The 100,000-year CH_4 signal is derived mainly from the effect of eccentricity modulation of precession on tropical monsoons and on methane generation in tropical wetlands. For the most part, each 23,000-year CH_4 maximum can be interpreted as a fast response to insolation values at that specific precession maximum, rather than to ice sheet suppression of methane generation (Fig. 4). Filtering the CH_4 signal detects power at 100,000 years because strong CH_4 maxima at the precession period are not balanced by comparable CH_4 minima. But the CH_4 signal has relatively little 100,000-year power and lacks the saw-toothed shape common to many 100,000-year climatic responses, so it is probably a secondary factor in global 100,000-year climatic responses.

In contrast, because 100,000-year power dominates the CO_2 signal and has a characteristic saw-toothed shape (Fig. 5), it is probably a major factor in projecting the 100,000-year response across the globe. Most of the 100,000-year power in the CO_2 signal probably originates from ice-sheet amplification of the obliquity signal. Ice sheets only grow large enough to drive a large CO_2 feedback during times when eccentricity modulation of precession is weak. In effect, this suppresses the 41,000-year CO_2 signal at the interglacial extreme, but allows strong maxima to develop at the glacial extreme, thus creating a 100,000-year CO_2 signal (Figs. 15 and 16).

The contribution of precession to the 100,000-year CO_2 signal may be indirect. The CO_2 maxima that occur every 23,000 years help drive climate into an interglacial state in which ice sheets remain small. If large ice sheets cannot grow, the strong 41,000-year CO_2 feedback cannot be activated, and CO_2 values will remain near the interglacial extreme. In this sense, the interglacial extreme of the 100,000-year CO_2 cycle is in part also a result of the 23,000-year CO_2 changes.

Finally, the 100,000-year hypothesis proposed here has implications for the timing of temperature overprints on the $\delta^{18}O$ signal. Previous studies concluded that a cold SST overprint began at major glacial–interglacial transitions between marine Isotopic Substages 5.5 and 5.4 and between Stages 5 and 4 (Chappell and Shackleton, 1986; Labeyrie et al., 1987), remained in place through the glaciation, and ended during the termination. In contrast, the analysis here implies that SST overprints are likely to have been added and subtracted to marine $\delta^{18}O$ signals on every orbital-scale oscillation. At the 23,000-year precession cycle, greenhouse gases should imprint artificially warm temperatures on the $\delta^{18}O$ signal during each ice-melt transition (including terminations), but then withdraw this overprint as ice grows in response to the next precessional decrease in insolation. For obliquity, the 41,000-year CO_2 cycle should overprint artificially cold temperatures during each 41,000-year ice-volume maximum during times of low eccentricity, but then withdraw this overprint early on the terminations.

7.2. Onset of the 100,000-year cycle

Long-term cooling is a plausible explanation for the appearance of the 100,000-year cycle in climate records near 0.9 Myr ago. Benthic foraminifera from the eastern Pacific (Mix et al., 1995) reveal a gradual $\delta^{18}O$ increase over the last 4.5 million years (Fig. 18). Because this signal is free from overprints of northern hemisphere ice volume prior to 2.75 million years ago, the 0.5‰ increase in mean $\delta^{18}O$ values is equivalent to a temperature decrease of 2.1°C in 1.75 Myr. Because deep-Pacific water originates in the Antarctic, this trend shows that a gradual cooling was underway at high southern latitudes. A similar long-term $\delta^{18}O$ trend that continued until 0.9 Myr indicates continued cooling, but with an ice-volume overprint as well.

Raymo (1997) proposed a mechanism to explain the appearance of the 100,000-year ice-volume signal near 0.9 Myr ago. She suggested that just prior to that time temperatures at high northern latitudes were cold enough to let ice sheets grow at many 41,000-year and 23,000-year insolation minima, but were still warm enough to melt all of that ice during the next insolation maximum. As a result, ice sheets grew and melted only at those periods (Raymo et al. 1989). Near 0.9 Myr, she proposed that northern hemisphere temperature cooled to a threshold that allowed some ice to persist through weak insolation maxima and reach a larger size. Building on an idea that was implicit in Broecker (1984), Raymo proposed that this process would tend to produce a 100,000-year cycle, because ice sheets would persist through clusters of low-amplitude insolation maxima at the precession period, but then melt during the next group of high-amplitude precession maxima. Because high-amplitude precession maxima occur every 100,000 years due to eccentricity modulation, ice sheets would tend to grow and melt with a period of 100,000 years.

The synthesis presented here accepts this basic explanation but adds another factor that should have contributed to the emergence of a 100,000-year signal. When ice sheets grew larger after 0.9 Myr ago, they would have begun to drive stronger 41,000-year responses in ice-proximal signals like dust fluxes,

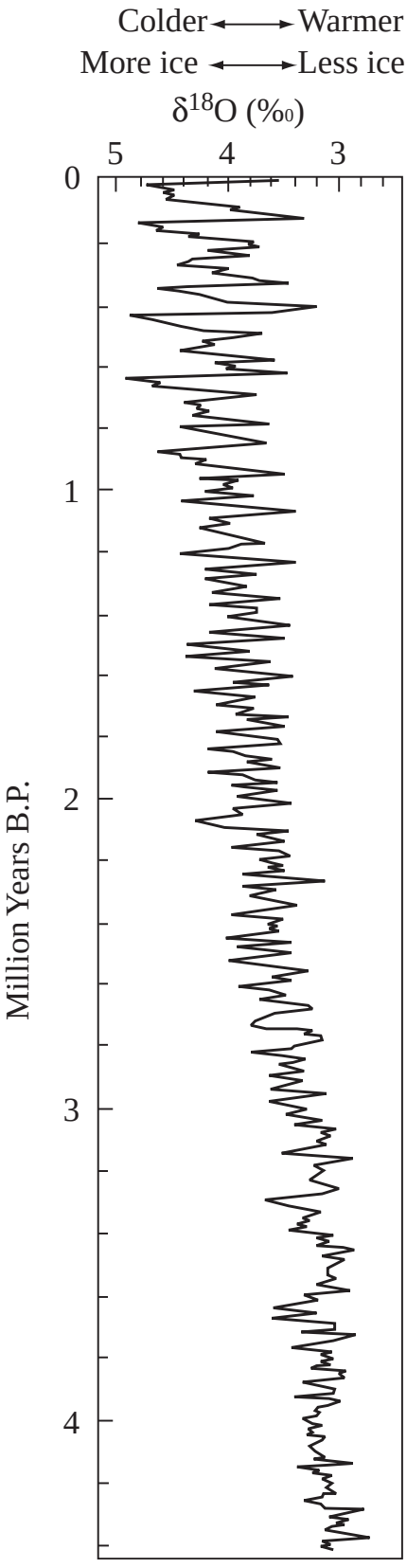

Fig. 18. Changes in $\delta^{18}O$ over the last 4.5 million years show a steady increase caused by decreased deep-water temperatures and increased ice volume (Mix et al., 1995).

NADW, and North Atlantic SST. These responses in turn would have amplified the 41,000-year CO_2 cycle to the point that it could provide feedback to the 100,000-year ice-volume signal. Prior to 0.9 Myr ago, 41,000-year responses were already visible in all of these ice-proximal responses: dust (Kukla et al., 1990), NADW (Raymo et al., 1990), and North Atlantic SST (Ruddiman et al., 1986). These signals probably provided some CO_2 feedback to the ice sheets, but only on individual 41,000-year cycles of ice growth. Only after 0.9 Myr ago would they have produced a feedback strong enough to help create the 100,000-year cycle.

7.3. The "Stage 11" problem and the issue of 400,000-year eccentricity forcing

Any hypothesis that ties the origin of the 100,000-year cycle to eccentricity modulation runs into the "Stage 11 problem" (also called the "400 K problem"). Time-dependent numerical models that generate 100,000-year signals from insolation forcing at the periods of obliquity and precession (Imbrie and Imbrie, 1980; Bassinot et al., 1994) encounter four problems linked to the 400,000-year eccentricity cycle that also modulates precession along with the 100,000-year cycle.

One problem is the absence of larger-than-normal interglaciations in the $\delta^{18}O$ record during times of very high eccentricity every 400,000 years (Fig. 17). The same mechanisms that cause major ice-volume minima at the 100,000-year cycle during large 23,000-year insolation maxima should cause even larger ice-volume minima at the 400,000-year cycle (for example between 100,000 and 300,000 years ago). The reason these abnormally large interglaciations are not observed in the $\delta^{18}O$ record is that the ice-volume signal is naturally rectified at or near its present-day limit: once the climate system has gotten rid of all the "vulnerable" ice on North America and Eurasia (and perhaps some of the ice on Greenland), it has reached a natural limit.

The converse problem is why larger ice sheets failed to grow larger during times of very low eccentricity at the 400,000-year cycle. In this case, the most likely explanation is inherent in the processes at work in the 100,000-year cycle. Ice accumulation even at cold temperatures is a slower process than ice ablation at warm temperatures (Oerlemans, 1991). As a result, melting during strong 23,000-year insolation maxima outstrips accumulation during even the deepest intervening insolation minima. As a result, ice sheets cannot grow larger at the longer 400,000-year cycle.

The remaining problems pertain to changes at the Isotopic Stage 12/11 boundary near 420,000 years ago (Fig. 17). The large $\delta^{18}O$ (ice-volume) maximum at Isotopic Stage 12 just before this deglaciation does not actually appear to be a problem: all precessional insolation minima during the preceding

50,000 years were very low in amplitude, so that ice sheets had avoided major melting events and had been able to grow to large size. In addition, ice volume had not been reduced to full-interglacial levels during Isotopic Stages 15 and 13, and a large amount of "carry-over" ice existed at the end of Stage 13 as a basis on which to build large ice sheets by the Stage 12 ice maximum

The main problems at the Stage 12/11 boundary are the size of the deglaciation and the unusual duration of the Stage 11 interglaciation that followed. These responses cannot easily be explained by orbital forcing, because the insolation maximum at high northern latitudes that coincides with the later part of the Stage 12/11 boundary is weak, yet the deglaciation is large.

Two arguments suggest that a problem may not actually exist. First, the fact that northern hemisphere ice-volume is naturally rectified at its interglacial extreme (the point at which it has all disappeared) strongly implies that the forcing available on some terminations could have melted more ice than was actually available. The very fast rates of deglaciation across the Stages 6/5 and 10/9 isotopic transitions suggest that Terminations II and IV are good candidates for times when additional ice would have been melted. If "excess forcing" was available on those terminations, the implication is that smaller amounts of insolation forcing might still have been able to melt all the vulnerable ice at other terminations like the Stage 12/11 (and 2/1) boundary.

Second, numerical models may have underestimated the contribution of obliquity. Even though precessional insolation reached a very weak maximum at the Stage 12/11 deglaciation, obliquity was passing through an unusually large and extended maximum (Berger and Loutre, 1992). If insolation forcing has an "excess" (unutilized) capacity to drive some deglaciations, then this large obliquity maximum in combination with a weak precession maximum may have been enough to melt all the ice. This suggestion finds support in the smooth rounded shape of the SPECMAP $\delta^{18}O$ signal (and other climatic responses) at the end of the Stage 12/11 deglaciation. This shape implies the kind of ice response expected for forcing from a large, extended obliquity maximum.

An alternative, but less appealing, explanation is that something internal to the climate system caused the Stage 12/11 deglaciation. One possibility is that the build-up of unusual volumes of ice by Isotopic Stage 12 had created unusually large amounts of "vulnerable" ice (marine ice shelves) in both hemispheres (Scherer, 1991). In this case, a moderate forcing toward deglaciation might have attacked an unusually large volume of ice by means of sea-level rise and ice-sheet destabilization, possibly altering CO_2 feedbacks in an anomalous way. Unfortunately, the Vostok ice record ends just above this critical interval, so that no CO_2 record of this deglaciation exists.

8. The last 10,000 years: anomalous trends in CH_4, Co_2 and ice volume

Orbital-scale phase relationships between insolation, ice volume, and greenhouse gases can be traced into the last 15,000 years (Fig. 19). Only changes of obliquity and precession are shown, because the 100,000-year climate cycle has been hypothesized here to result from amplification of forced changes at these two cycles. Mid-July orbital precession reached a maximum value near 11,000 years ago, and obliquity reached a maximum near 10,000 years ago (Fig. 19, top).

The phase relationships shown in Figs. 10 and 12 predict the timing (although not the magnitude) of

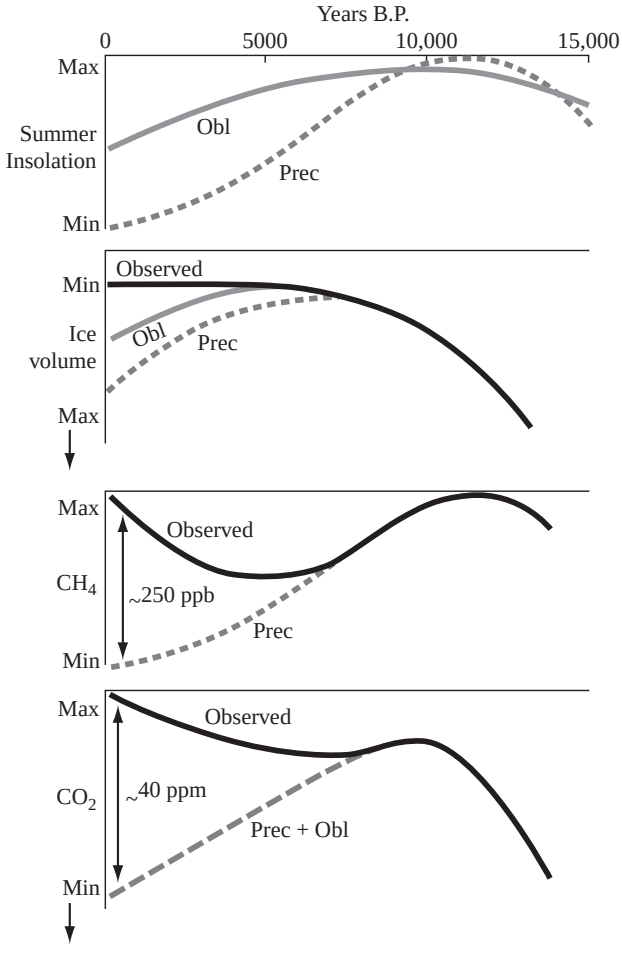

Fig. 19. (Top) Ice volume followed the projected orbital-scale behavior from 15,000 until 6000 years ago, after which ice failed to grow as predicted. (Center to Bottom) Both CH_4 and CO_2 followed the projected orbital-scale behavior until 5000 and 8000 years ago (respectively), after which the concentrations of both gases increased instead of continuing to decrease as predicted.

ice-sheet changes over the last 10,000 years. For orbital precession, with ice volume lagging 4500 years behind insolation, ice sheets should have reached a minimum 6500 years ago and then begun to grow. For obliquity, the 6500-year ice-volume lag behind insolation forcing should have produced ice-sheet growth after 3500 years ago. The deglacial portion of the observed ice-volume trend appears to be in reasonable agreement with these predictions. The European ice sheet had melted by about 10,000 years ago, and North American ice by 6000 years ago (Clark and Mix, 2002). But no accumulation of global ice has occurred in the last several millennia, and this disagrees with the predictions based on long-term trends.

The phase relationships summarized in Figs. 10 and 12 also predict patterns of change in the greenhouse gases. At the precession cycle, both the CH_4 and CO_2 concentrations should have reached peaks near 11,000 years ago and then steadily declined until today. At the obliquity cycle, the CO_2 decrease should have begun near 3500 years ago, the time ice sheets should have begun to grow. The observed greenhouse-gas trends initially match these expected patterns, but then they diverge. CH_4 reached a peak near 11,000 years ago and then decreased by 100 ppb until 5000 years ago (Blunier et al., 1995), but then it began a totally unpredicted rise (of 100 ppb) prior to the industrial era. The CO_2 signal reached a peak after 11,000 years ago and slowly fell until 8000 years ago (Indermuhle et al., 1999), but then it also began an unpredicted increase of 20–25 ppm.

In summary, the observed greenhouse-gas trends match those predicted from longer-term orbital relationships prior to 8000–5000 years ago, but then begin anomalous rises. And northern hemisphere ice sheets that should have begun to grow several thousand years ago failed to appear, even though decreasing summer insolation in the northern hemisphere favored ice growth. These anomalous responses point to an obvious connection: whatever caused greenhouse gases to begin their "anomalous" rises countered the insolation trends and stopped the ice sheets from growing.

Ruddiman and Thomson (2001) noted that the two proposed natural explanations of the CH_4 rise since 5000 years ago (greater CH_4 input from tropical wetlands or boreal peat-lands) can be rejected based on other evidence. They concluded that human activities must be responsible for the anomalous methane production. Human populations had begun to increase as a result of the discovery of agriculture 12,000 years ago, and tending of livestock and cultivation of rice had begun between 8000 and 6500 years ago. Although the number of humans on Earth 5000 years ago was still very small relative to today's population, methane emissions were an unavoidable product of daily activity such as tending livestock (which generate CH_4 by waste and gastric emissions), human waste, biomass burning, and (especially) irrigation for rice, which began 5000 years ago.

Ruddiman (ms submitted) noted that the CO_2 rise since 8000 years ago differs from the trends observed for the three previous interglaciations, all of which record uninterrupted CO_2 decreases for at least 15,000 years after late-deglacial CO_2 maxima (Fig. 5). He also rejected the only two published explanations for the CO_2 rise, both based on natural processes. Indermuhle et al. (1999) concluded that the CO_2 increase was caused by a large natural loss of terrestrial biomass, but Ruddiman cited evidence from ecosystem modeling by Foley (1994) showing negligible global-mean changes in carbon biomass between 6000 years ago and today from natural (insolation-driven) forcing. Broecker et al. (1999) suggested that changes in ocean carbonate chemistry resulting from deglacial reforestation might explain the CO_2 trends, but Ruddiman rejected this explanation because no comparable CO_2 rise occurred on the three previous deglaciations, even though virtually identical deglacial reforestations occurred in each case.

Ruddiman (submitted) proposed an anthropogenic origin for the CO_2 rise since 8000 years ago. Evidence summarized by Roberts (1998) shows that humans began to cut forests for agriculture in Europe just as the anomalous CO_2 increase began. By 2000 years ago, complex agricultural practices had replaced natural forests in large areas of southern and western Europe, India, and eastern China. Early deforestation in these regions is more than large enough to account for the observed increase in CO_2 since 8000 years ago. Ruddiman estimated the full amplitude of the anthropogenic inputs at 250 ppb for CH_4 and 40 ppm for CO_2. These estimates incorporated both the observed increases of these greenhouse gases as well as the amount by which the concentrations should have decreased during the last several thousand years but did not (Fig. 19).

These anthropogenic anomalies would produce a radiatively forced warming of about 0.8°C globally for a global climatic sensitivity to a CO_2 doubling of 2.5°C. With positive albedo feedback at high latitudes, the warming should be about 2.5 times larger, or 2°C. Based on energy-balance modeling, Williams (1978) reported that broad areas of high terrain in northeast Canada were within 1°C to 2°C of the glaciation limit during the Little Ice Age. Without the early anthropogenic warming of 2°C, large parts of northeast Canada would have been cold enough for an ice sheet to grow. In summary, human additions of greenhouse gases to the atmosphere since 8000 to 5000 years ago have been large enough to stop a glaciation that would have been produced by natural trends of falling summer insolation and decreasing greenhouse-gas concentrations.

References

Bard, E., Hamelin, B., Fairbanks, R.F., 1990. U-Th ages obtained by mass spectrometry in corals from Barbados: sea level during the past 130,000 years. Nature 346, 456–458.

Bard, E., Rostek, F., Conzogni, C., 1997. Interhemispheric Synchrony of the last deglaciation inferred from alkenone palaeothermometry. Nature 385, 707–710.

Bassinot, F.C., Labeyrie, L.D., Vincent, E., Quidelleur, X., Shackleton, N.J., Lancelot, Y., 1994. The astronomical theory of climate and the age of the Brunhes/Matuyama magnetic reversal. Earth and Planetary Science Letters 126, 91–108.

Bender, M., Sowers, T., Labeyrie, L., 1994. The Dole effect and its variations during the last 130,000 years as measured in the Vostok ice core. Global Biogeochemical Cycles 8, 363–376.

Berger, A., Loutre, M.F., 1992. Astronomical solutions for paleoclimate studies over the last 3 million years. Earth and Planetary Science Letters 111, 369–392.

Blunier, T., Chappellaz, J., Schwander, J., Stauffer, J., Raynaud, D., 1995. Variations in atmospheric methane concentration during the Holocene epoch. Nature 374, 46–49.

Bond, G., Broecker, W.S., Johnsen, S.J., McManus, J., Labeyrie, L.D., Jouzel, J., Bonani, G., 1993. Correlations between climatic records from North Atlantic sediments and Greenland ice. Nature 365, 143–147.

Boyle, E.A., 1984. Cadmium in benthic foraminifera and abyssal hydrography: evidence for a 41 kyr obliquity cycle. In: Hansen, J.E., Takahashi, T. (Eds.), Climate Processes and Climate Sensitivity, Geophysical Monograph Series, Vol. 29. AGU, Washington, DC, pp. 360–368.

Boyle, E.A., 1992. Cadmium and $\delta^{13}C$ paleochemical ocean distributions during the Stage 2 glacial maximum. Annual Reviews of Earth and Planetary Science 20, 245–287.

Brathauer, U., Abelmann, A., 1999. Late Quaternary variations in sea surface temperatures and their relationship to orbital forcing recorded in the Southern Ocean (Atlantic sector). Paleoceanography 14, 135–148.

Broecker, W.S., 1979. A revised estimate of the radiocarbon age of North Atlantic Deep Water. Journal of Geophysical Research 82, 2218–2226.

Broecker, W.S., 1982. Glacial to interglacial changes in ocean chemistry. Progress in Oceanography 11, 151–197.

Broecker, W.S., 1984. Terminations. In: Berger, A.L., et al. (Ed.), Milankovitch and Climate. Reidel, Dordrecht, pp. 687–698.

Broecker, W.S., Denton, G.H., 1989. The role of ocean–atmosphere reorganizations in glacial cycles. Geochimica et Cosmochimica Acta 53, 2465–2501.

Broecker, W.S., Peng, T.-H., 1989. The cause of the glacial to interglacial atmospheric CO_2 change: a polar alkalinity hypothesis. Global Biogeochemical Cycles 3, 215–239.

Broecker, W.S., Clark, E., McCorckle, D.C., Peng, T.-H., Hajdas, I., Bonani, G., 1999. Evidence for a reduction in the carbonate ion content of the deep sea during the course of the Holocene. Paleoceanography 3, 317–342.

Chappell, J.M.A., Shackleton, N.J., 1986. Oxygen isotopes and sea level. Nature 324, 137–138.

Chappellaz, J., Barnola, J.-M., Raynaud, D., Korotkevitch, Y.S., Lorius, C., 1990. Atmospheric CH_4 record over the last climatic cycle revealed by the Vostok ice core. Nature 345, 127–131.

Clark, P.U., Mix, A.C., 2002. Ice sheets and sea level of the Last Glacial Maximum. Quaternary Science Reviews 21, 1–8.

Clemens, S.C., Prell, W.L., 1990. Late Pleistocene variability of Arabian Sea summer monsoon winds and continental aridity: eolian records from the lithogenic component of deep-sea sediments. Paleoceanography 5, 109–145.

Clement, A.C., Cane, M.A., Seager, R., 2001. An orbitally driven tropical source for abrupt climate change. Journal of Climate Change 14, 2369–2375.

Dansgaard, W., Johnsen, S.J., Clausen, H.B., Dahl-Jensen, D., Gundestrup, N., Hammer, C.U., Oeschger, H., 1984. North Atlantic climate oscillations revealed by deep Greenland ice cores. In: Hansen, J.E., Takahashi, T. (Eds.), Climate Processes and Climate Sensitivity, Geophysical Monograph Series, Vol. 29. AGU, Washington, DC, pp. 288–298.

Edwards, R.L., Chen, J.H., Ku, T.-L., Wasserburg, G.J., 1987. Precise timing of the last interglacial period from mass-spectrometric determination of Thorium-230 in corals. Science 236, 1547–1553.

Foley, J.A., 1994. The sensitivity of the terrestrial biosphere to climatic change: a simulation of the middle Holocene. Global Biogeochemical Cycles 8, 505–525.

Gardner, J.V., Hays, J.D., 1976. Responses of sea-surface temperature to global climatic change during the past 200,000 years in the eastern Equatorial Atlantic. Geological Society of America Memoir 145, 221–246.

Genthon, C., Barnola, J.M., Raynaud, D., Lorius, C., Jouzel, J., Barkov, N.I., Korotkevitch, Y.S., Kotlyakov, V.M., 1987. Vostok ice core: climatic response to CO_2 and forcing changes over the last climatic cycle. Nature 329, 414–418.

Hays, J.D., Imbrie, J.I, Shackleton, N.J., 1976a. Variations in the earth's orbit: pacemaker of the ice ages. Science 194, 1121–1132.

Hays, J.D., Lozano, J.A., Shackleton, N.J., Irving, G., 1976b. Reconstruction of the Atlantic and western Indian Ocean sectors of 18,000 BP Antarctic Ocean. Geological Society of America Memoir 145, 337–372.

Hovan, S.A., Rea, D.K., Pisias, N.G., Shackleton, N.J., 1989. A direct link between the China loess and marine $\delta^{18}O$ records: aeolian flux to the north pacific. Nature 340, 296–298.

Imbrie, J., Imbrie, J.Z., 1980. Modeling the climatic response to orbital variations. Science 207, 943–953.

Imbrie, J., et al., 1984. The orbital theory of Pleistocene climate: support from a revised chronology of the marine $\delta^{18}O$ record. In: Berger, A.L., et al. (Ed.), Milankovitch and Climate, Part I. D. Reidel, Dordrecht, pp. 269–305.

Imbrie, J., McIntyre, A., Mix, A., 1989. Oceanic response to orbital forcing in the late Quaternary: observational and experimental strategies. In: Berger, A.L., et al. (Ed.), Climate and Geo-Sciences. Kluwer Academic Publication, Dordrecht, pp. 121–164.

Imbrie, J., Boyle, E.A., Clemens, S.C., Duffy, A., Howard, W.R., Kukla, G., Kutzbach, J., Martinson, D.G., McIntyre, A., Mix, A.C., Molfino, B., Morley, J.J., Peterson, L.C., Pisias, N.G., Prell, W.L., Raymo, M.E., Shackleton, N.J., Toggweiler, J.R., 1992. On the structure and origin of major glaciation cycles. I. Linear responses to Milankovitch forcing. Paleoceanography 7, 701–738.

Imbrie, J., Berger, A., Boyle, E.A., Clemens, S.C., Duffy, A., Howard, W.R., Kukla, G., Kutzbach, J., Martinson, D.G., McIntyre, A., Mix, A.C., Molfino, B., Morley, J.J., Peterson, L.C., Pisias, N.G., Prell, W.L., Raymo, M.E., Shackleton, N.J., Toggweiler, J.R., 1993. On the structure and origin of major glaciation cycles. II. The 100,000-year cycle. Paleoceanography 8, 699–735.

Indermuhle, A., Stocker, T.F, Joos, F., Fischer, H., Smith, H.J., Wahlen, M., Deck, B., Masttroianni, D., Blunier, T., Meyer, R., Stauffer, B., 1999. Holocene carbon-cycle dynamics based on CO_2 trapped in ice at Taylor Dome, Antarctica. Nature 398, 121–126.

Jenkins, G.M., Watts, D.G., 1968. Spectral Analysis and its Applications. Holden Day, San Francisco, 525pp.

Jouzel, J., Lorius, C., Petit, J.R., Genthon, C., Barkov, N.I., Kotlyakov, V.M., Petrov, V.N., 1990. Vostok ice core: a

continuous isotope temperature record over the last climatic cycle (160,000 years). Nature 329, 403–409.

Jouzel, J., Barkov, N.I., Barnola, J.M., Bender, M., Chappellaz, J., Genthon, C., Kotlyakov, V.M., Lipenkov, V., Lorius, C., Petit, J.R., Raynaud, D., Raisbeck, G., Ritz, C., Sowers, T., Stievenard, M., Yiou, F., Yiou, P., 1993. Extending the Vostok ice-core record of paleoclimate to the penultimate glacial period. Nature 364, 407–412.

Keigwin, L.D., Boyle, E.A., 1999. Surface and deep ocean variability in the northern Sargasso sea during marine isotope Stage 3. Paleoceanography 14, 164–170.

Keigwin, L.D., Lehman, S.J., 1994. Deep circulation change linked to Heinrich Event 1 and Younger Dryas in a middepth North Atlantic core. Paleoceanography 9, 185–194.

Kukla, G., An, S., Melice, J.L., Gavin, J., Xiao, J.L., 1990. Magnetic susceptibility record of Chinese loess. Transactions of the Royal Society of Edinburgh Earth Science 81, 263–288.

Kutzbach, J.E., 1981. Monsoon climate of the early Holocene: climate experiment with earth's orbital parameters for 9000 years ago. Science 214, 59–61.

Labeyrie, L.D., Duplessy, J.-C., Blanc, P.L., 1987. Variations in mode of formation and temperature of oceanic waters over the past 125,000 years. Nature 327, 477–482.

Labeyrie, L.D., et al., 1996. Hydrographic changes of the Southern Ocean (southeast Indian sector) over the last 230 kyr. Paleoceanography 11, 57–76.

Lea, D.W., Pak, D.L., Spero, H.J., 2000. Climatic impact of late Quaternary east Pacific sea-surface temperature variation. Science 289, 1719–1724.

Manabe, S., Broccoli, A.J., 1985. The influence of continental ice sheets on the climate of an Ice Age. Journal of Geophysical Research 90, 2167–2190.

Martin, J.H., 1990. Glacial–interglacial CO_2 changes: the iron hypothesis. Paleoceanography 5, 1–13.

Mayewski, P.A., Twickler, M.S., Whitlow, S.I., Meeker, L.D., Yang, Q., Thomas, J., Kreutz, K., Grootes, P.M., Morse, D.L., Steig, E.J., Waddington, E.D., Saltzman, E., Whung, P.-Y., Taylor, K.C., 1996. Climate change during the last deglaciation in Antarctica. Science 272, 1636–1637.

McIntyre, A., Ruddiman, W.F., Karlin, K., Mix, A.C., 1989. Surface water response of the equatorial Atlantic Ocean to orbital forcing. Paleoceanography 4, 19–55.

Milankovitch, M., 1941. Kanon der Erdbestrahlung und seine Andwendung auf das Eiszeitenproblem, Vol. 133. Royal Serbian Academy Special Publication, Belgrade, 633pp. (English translation published in 1969 by Israel Program for Scientific Translations, US Dept. Comm.)

Mix, A.C., 1989. Influence of productivity variations on long-term atmospheric CO_2. Nature 337, 541–544.

Mix, A.C., 1996. Climate feedback and Pleistocene variations in the Atlantic South Equatorial Current. In: Wefer, G., Berger, W.H., Siedler, G., Webb, D.J. (Eds.), The South Atlantic: Present and Past Circulation. Springer, Berlin, pp. 503–525.

Mix, A.C., Ruddiman, W.F., McIntyre, A., 1986. Late Quaternary Paleoceanography of the tropical Atlantic, I: spatial variability of annual mean sea-surface temperatures, 0–20,000 years B.P. Paleoceanography 1, 43–66.

Mix, A.C., Pisias, N.G., Rugh, W., Wilson, J., Morey, A., Hagelberg, T.K., 1995. Benthic foraminifer stable isotope record from Site 849 (0–5 Ma): local and global climate changes. Proceedings of the Ocean Drilling Program 138, 371–412.

Mix, A., Bard, E., Schneider, R., 2001. Environmental processes of the Ice Age: land, oceans, glaciers (epilog). Quaternary Science Reviews 20, 627–657.

Nicholson, S.E., Flohn, H., 1981. African climatic changes in late Pleistocene and Holocene and the general atmospheric circulation. IAHS Publication 131, 295–301.

Oerlemans, J., 1991. The role of ice sheets in the Pleistocene climate. Norsk Geologisk Tiddskrift 71, 155–161.

Oppo, D.W., Rosenthal, Y., 1994. Cd/Ca changes in a deep Cape Basin core over the past 730,000 years: response of circumpolar deepwater variability to northern hemisphere ice sheet melting? Paleoceanography 9, 661–675.

Petit, J.R., Jouzel, J., Raynaud, D., Barkov, N.I., Barnola, J.-M., Basile, I., Bender, M., Chappellaz, J., Davis, M., Delaygue, G., Delmotte, M., Kotlyakov, V.M., Lipenkov, V., Lorius, C., Pepin, L., Ritz, C., Saltzman, E., Stievenard, M., 1999. Climate and atmospheric history of the last 420,000 years from the Vostok ice core, Antarctica. Nature 399, 429–436.

Pisias, N.G., Mix, A.C., Zahn, R., 1990. Nonlinear response in the global climate system: evidence from benthic oxygen isotopic record in core RC13-110. Paleoceanography 5, 147–160.

Prell, W.L., Kutzbach, J.E., 1987. Monsoon variability over the last 150,000 years. Journal Geophysical Research 92, 8411–8425.

Raymo, M.E., 1997. The timing of major climatic terminations. Paleoceanography 12, 577–585.

Raymo, M.E., Ruddiman, W.F., Backman, J., Clement, B.M., Martinson, D.M., 1989. Late Pliocene variation in northern hemisphere ice sheets and North Atlantic Deep Water circulation. Paleoceanography 4, 413–446.

Raymo, M.E., Ruddiman, W.F., Shackleton, N.J., Oppo, D.W., 1990. Evolution of Atlantic–Pacific $\delta^{13}C$ gradients over the last 2.5 m.y. Earth and Planetary Science Letters 97, 353–368.

Raymo, M.E., Oppo, D.W., Curry, W., 1997. The mid-Pleistocene climate transition: a deep-sea carbon perspective. Paleoceanography 12, 546–559.

Raynaud, D., Barnola, J.M., Chappellaz, J., Zardini, D., Jouzel, J., Lorius, C., 1992. Glacial–interglacial evolution of greenhouse gases as inferred from ice-core analysis: a review of recent results. Quaternary Science Reviews 11, 381–386.

Rind, D., Peteet, D., Broecker, W., McIntyre, A., Ruddiman, W., 1986. The impact of cold North Atlantic sea surface temperatures on climate: implications for the Younger Dryas. Climate Dynamics 1, 3–33.

Roberts, N., 1998. The Holocene. Blackwell Publishers, Oxford.

Ruddiman, W.F. The anthropogenic greenhouse era began thousands of years ago. Submitted to Climatic Change.

Ruddiman, W.F., McIntyre, A., 1984. Ice-age thermal response and climatic role of the surface North Atlantic ocean (40°N to 63°N). Geological Society of America Bulletin 95, 381–396.

Ruddiman, W.F., Raymo, M.E., 2003. A methane-based time scale for Vostok ice: Climatic implications. Quaternary Science Reviews 22, 141–155.

Ruddiman, W.F., Thomson, J.S., 2001. The case for human causes of increased atmospheric CH_4 over the last 5000 years. Quaternary Science Reviews 20, 1769–1777.

Ruddiman, W.F., Raymo, M.E., McIntyre, A., 1986. Matuyama 41,000-year cycles: North Atlantic Ocean and northern hemisphere ice sheets. Earth and Planetary Science Letters 80, 117–129.

Sarnthein, M., Winn, K., Duplessy, J.-C., Fontugne, M.R., 1988. Global variations of surface ocean productivity in low and mid latitudes: influence on CO_2 reservoirs of the deep ocean and atmosphere during the last 21,000 years. Paleoceanography 3, 361–399.

Scherer, R.P., 1991. Quaternary and Tertiary microfossils from beneath ice stream B: evidence for a dynamic West Antarctic ice sheet history. Palaeogeography, Palaeoclimatology, Palaeoecology 90, 395–412.

Schneider, R.R., Muller, P.J., Ruhland, G., 1995. Late Quaternary surface circulation in the east equatorial South Atlantic: evidence from Alkenone sea surface temperatures. Paleoceanography 10, 197–219.

Shackleton, N.J., 2000. The 100,000-year ice-age cycle identified and found to lag temperature, carbon dioxide, and orbital eccentricity. Science 289, 1897–1902.

Stephens, B.B., Keeling, R.F., 2000. The influence of Antarctic sea ice on glacial–interglacial CO_2 variations. Nature 404, 171–174.

Weertman, J., 1964. Rate of growth and shrinkage of non-equilibrium ice sheets. Journal of Glaciology 5, 145–158.

Williams, L.D., 1978. The Little Ice Age glaciation level on Baffin Island, Arctic Canada. Palaeogeography, Palaeoclimatology, Palaeoecology 25, 199–207.

Zwally, J., Comiso, J., Parkinson, C., Campbell, F., Carsey, F., Gloersen, P., 1983. Antarctic Sea Ice 1973–1976: Satellite Passive Microwave Variations. NASA SP 459, Washington, DC.